

Linker-Dependent Singlet Fission in Tetracene Dimers

Nadezhda V. Korovina, Jimmy Joy, Xintian Feng, Cassidy Feltenberger,
Anna I. Krylov, Stephen E. Bradforth, and Mark E Thompson

J. Am. Chem. Soc., **Just Accepted Manuscript** • DOI: 10.1021/jacs.8b04401 • Publication Date (Web): 17 Jul 2018

Downloaded from <http://pubs.acs.org> on July 17, 2018

Just Accepted

“Just Accepted” manuscripts have been peer-reviewed and accepted for publication. They are posted online prior to technical editing, formatting for publication and author proofing. The American Chemical Society provides “Just Accepted” as a service to the research community to expedite the dissemination of scientific material as soon as possible after acceptance. “Just Accepted” manuscripts appear in full in PDF format accompanied by an HTML abstract. “Just Accepted” manuscripts have been fully peer reviewed, but should not be considered the official version of record. They are citable by the Digital Object Identifier (DOI®). “Just Accepted” is an optional service offered to authors. Therefore, the “Just Accepted” Web site may not include all articles that will be published in the journal. After a manuscript is technically edited and formatted, it will be removed from the “Just Accepted” Web site and published as an ASAP article. Note that technical editing may introduce minor changes to the manuscript text and/or graphics which could affect content, and all legal disclaimers and ethical guidelines that apply to the journal pertain. ACS cannot be held responsible for errors or consequences arising from the use of information contained in these “Just Accepted” manuscripts.

Linker-Dependent Singlet Fission in Tetracene Dimers

Nadezhda V. Korovina^{††}, Jimmy Joy[†], Xintian Feng[§], Cassidy Feltenberger, Anna I. Krylov,

Stephen E. Bradforth* and Mark E. Thompson*

Department of Chemistry, University of Southern California, Los Angeles, California 90089, United States

KEYWORDS Singlet fission, dimers, tetracene, femtosecond spectroscopy, cyclic voltammetry

ABSTRACT: Separation of triplet excitons produced by singlet fission is crucial for efficient application of singlet fission materials. While earlier works explored the first step of singlet fission – the formation of the correlated triplet pair state, the focus of recent studies has been on understanding the second step of singlet fission – the formation of independent triplets from the correlated pair state. We present the synthesis and excited state dynamics of meta- and para-bis(ethynyltetracenyl)benzene dimers that are analogues to the ortho-bis(ethynyltetracenyl)benzene dimer reported by our groups previously. A comparison of the excited-state properties of these dimers allows us to investigate the effects of electronic conjugation and coupling on singlet fission between the ethynyltetracene units within a dimer. In the para isomer, in which the two chromophores are conjugated, the singlet exciton yields the correlated triplet pair state, from which the triplet excitons can decouple via molecular rotations. Contrastingly, the meta isomer in which the two chromophores are cross-coupled, predominantly relaxes via radiative decay. We also report the synthesis and excited-state dynamics of two para dimers with different bridging units joining the ethynyltetracenes. The rate of singlet fission is found to be faster in the dimer with the bridging unit that has orbitals closer in energy to that of the ethynyltetracene chromophores.

INTRODUCTION

Singlet fission is a process in which a singlet (S_1) excited state of a molecule shares energy with a neighboring chromophore, yielding a pair of triplet (T_1) excitons.^{1,3} Incorporation of such materials in organic solar cells could improve the power conversion efficiencies by doubling the number of excitons generated by high energy photons, thereby averting thermal losses. Hanna and Nozik have reported that the Shockley-Queisser limit – the theoretical power conversion efficiency limit of 33% for a single junction device – could be increased up to 44.4% by combining an efficient singlet fission material with a red absorber in a device⁴ while Tayebjee et al. take endothermic fission into account to derive an efficiency of 45.9%.⁵ In the seminal work of Congreve *et al.*, an internal quantum efficiency of 160% was demonstrated in a pentacene/poly(3-hexylthiophene) device⁶; however, the power conversion efficiencies of most singlet fission devices are sub-optimal, which leaves room for improvement in regard to material design.

An important criterion for singlet fission materials for solar cell utilization is fast rate of fission, to ensure that charge injection occurs from the triplet state, rather the singlet state; particularly, singlet fission rates faster than 100 ps are desirable.⁷ The rate of singlet fission is proportional to the square of the coupling term: $\langle S_1 S_0 | \hat{H}_{el} | ^1(T_1 T_1) \rangle$ between the $[S_1 S_0]$ state and the biexciton state, often described as correlated triplet pair [$^1(T_1 T_1)$], and is also dependent on the energy gap between these states.⁸ Early models by Smith and Michl suggested that $\langle S_1 S_0 | \hat{H}_{el} | ^1(T_1 T_1) \rangle$ is maximized in slip-stacked, π -overlapping arrangements of the chromophores¹ however, more sophisticated theoretical treatments³ show that coupling can also be significant in sandwiched and even coplanar chromophores.^{3,9,10}

The effect of the electronic coupling on singlet fission is best demonstrated using covalently-coupled chromophores (such as dimers and larger arrays).¹¹⁻¹⁷ Analysis of the excited-state dynamics of dimers in solution is advantageous because it allows one to separate the effects of coupling from the solid-state effects (such as intermolecular exciton delocalization) on the rates of singlet fission. Substantial progress has been made toward the synthesis and photophysical characterization of acene dimers and larger arrays, as well as in covalently linked systems of other singlet fission chromophores.¹⁸⁻³⁶ Efficient singlet fission has been reported in dimers wherein the constituent chromophores exhibit substantial π orbital overlap, or are linked together in a conjugated manner; conversely, dimers in which the chromophores are cross-conjugated exhibit slower singlet fission. Guldi *et al.* have reported fast and efficient singlet fission in *ortho*-, *meta*- and *para*-TIPS-pentacene dimers, in which the favorable energy(S_1) $\geq 2 \times$ energy(T_1) alignment provides the enthalpic driving force for fission, such that even the weakly coupled *meta* pentacene dimers exhibited singlet fission on picosecond timescales.^{19,37} In dimers of tetracene and diphenylisobenzofuran, in which the chromophores are without any significant π orbital overlap or conjugation, and are out of plane with respect to each other, singlet fission was reported to be slow and inefficient, likely due to weak coupling and the energy(S_1) $\leq 2 \times$ energy(T_1) energy alignment.³⁸⁻⁴⁰ Recent work on singlet fission with pentacene has also explored the role of conformational dynamics in facilitating excited state processes,⁴¹ observing the correlated triplet pair state with mid-IR spectroscopy⁴² and polarization resolved transient absorption microscopy,⁴³ and using electron paramagnetic resonance⁴⁴ and femtosecond stimulated Raman spectroscopy⁴⁵ as probes for singlet fission. Ito et al. have theoretically studied how the next-nearest-neighbor interactions affect singlet fission in *ortho*-, *meta*- and *para*-pentacene dimers⁴⁶ while

Zeng has used quantum dynamical simulations to explore the role of through bond coupling in singlet fission dimers.⁴⁷

The currently accepted mechanistic picture of singlet fission involves an intermediate biexciton state⁴⁸, which can be described as a correlated triplet pair [$^1(T_1T_1)$], connecting the singlet excited state [S_0S_1] with the two independent triplet states [3T_1].¹ Previously, we reported fast and efficient formation of the biexciton state in *ortho*-bis(ethynyltetracenyl)benzene (*o*-BETB), in which the two tetracene units are oriented in a twisted configuration with π -overlap and appear to be strongly electronically coupled – i.e. there is good coupling between the [S_0S_1] and the [$^1(T_1T_1)$] states. Although the π orbital overlap between the tetracenes provides significant through-space coupling, *ab initio* calculations showed that the conjugating, *ortho*-diethynylbenzene linker also contributes to the coupling, i.e., via through-bond mechanism.⁴⁹ To disentangle the role of through-bond *versus* through-space coupling we synthesized the *meta* and the *para* analogs of *ortho*-bis(ethynyltetracenyl)benzene (*m*-BETB, *p*-BETB-ehex and *p*-BETB-ohex, Figure 1). The position of the alkyne substitution on the benzene ring heavily influences the ground state electronic structure of molecules containing these diethynylbenzene units.⁵⁰ In the *ortho* and the *para* isomers, the π -systems of the two chromophores are conjugated, which leads to through-bond contributions to the coupling, whereas in the *meta* isomer the linker does not facilitate conjugation between the tetracene units that are pendant on the alkynes, resulting in only small through-space coupling. The conjugation through the linkers can be understood in terms of the cumulene-like resonance form of the *ortho*- and *para*-diethynylbenzenes.^{51, 52} Importantly, the conjugation manifest itself in strong interactions between the chromophores both in the ground and in the excited state. The *para*-diethynylbenzene particularly facilitates efficient electronic communication between the chromophores it bridges;⁵³⁻⁵⁵ as a result, compounds based on this chemical motif have been incorporated into ultrasensitive sensors,⁵⁶ energy harvesting materials,⁵⁷ and molecular electronic devices.^{58, 59} The *meta*-diethynylbenzene is cross-conjugating and has been demonstrated to provide only weak coupling between the chromophores tethered to it.^{60, 61} Calculations of tetracene-based dimers and model structures have shown that the linker contributes significantly to the coupling, via through-bond interaction, which affects the character of the states involved in singlet fission.⁶²⁻⁶⁴ A recent theoretical work by Abraham and Mayhall provides a model for determining the effect of the covalent linker on the boundedness of the $^1(T_1T_1)$ state based on Ovchinnikov rule. They concluded that the *ortho*- and *para*-benzene dimers of ethynylpentacene and

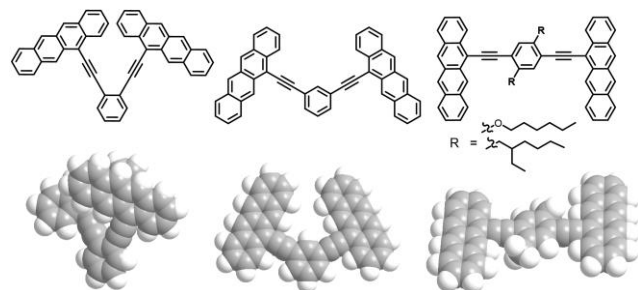
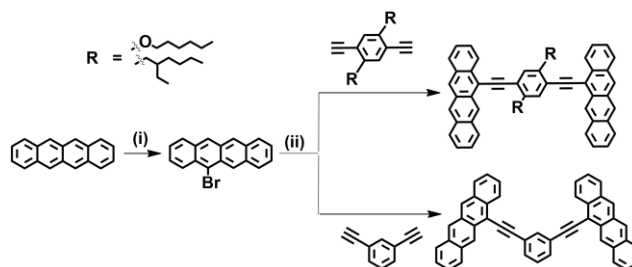


Figure 1. The chemical (top row) and space filling structures (bottom row) of *o*-BETB, *m*-BETB, and *p*-BETB-ehex and *p*-BETB-ohex. Two *para* dimers with different substituents on the linker were synthesized (*p*-BETB-ohex: R = OC₆H₁₃ and *p*-BETB-ehex: R = 2-(ethyl)hexyl).

ethynyltetracene have bound $^1(T_1T_1)$ states, whereas *meta* coupled dimers should have un-bound $^1(T_1T_1)$ states.⁶⁵ The boundedness of the $^1(T_1T_1)$ state is an important factor when considering the applications of singlet fission materials. The materials in which the $^1(T_1T_1)$ state is bound will not readily produce free triplet excitons, which are essential for reaping the benefits of singlet fission in devices. Therefore, it is valuable to understand the method by which the triplets can decouple from the initially formed biexciton state.

Although the favorable energy(S_1) $\geq 2 \times$ energy(T_1) energy alignment in the dimers reported by Guldi et al. ensured fast singlet fission, it was unresolvable with the instrument response of their transient absorption spectrometer in *ortho*, and *para* dimers and rapid annihilation to the ground state was observed. The isoenergetic energy(S_1) $\approx 2 \times$ energy(T_1) conditions in our bis(ethynyltetracenyl)benzene dimers result in singlet fission rates that are fast but still resolvable with our instrument response, and the dynamics of the population of each of the three states involved in singlet fission could be observed in our *para* dimers. In comparison to the tetracene dimers reported by Bardeen *et al.*, in which the acenes were directly attached to the phenyl linker and displayed slow singlet fission, the tetracene units in our dimers are connected to the phenyl linker via ethynyl groups. This ensures conjugation between the tetracenes (via the cumulene resonance structure) and less steric hindrance within a dimer, which could result in faster singlet fission.⁴⁰ The presence of ethynyl groups in our ethynyltetracene dimers also perturbs the S_1 and T_1 state energies in a favorable way, as evidenced by faster fission rates.⁴⁹ Using ultrafast spectroscopy, we observe that the *para*-bis(ethynyltetracenyl)benzene dimers (*p*-BETB-ohex: R = OC₆H₁₃ and *p*-BETB-ehex: R = 2-(ethyl)hexyl in Figure 1) undergo singlet fission form independent triplet states, whereas no significant singlet fission in the *meta*-bis(ethynyltetracenyl)benzene dimer (*m*-BETB) is observed. To understand the differences in the excited-state behavior of the *ortho* vs. the *para* dimers, we present the transient spectroscopy of *p*-BETB-ehex in THF and *p*-BETB-ehex suspended in a rigid polymer matrix (poly-(methylmethacrylate), PMMA) and model the kinetics using two populations that exhibit distinct excited state dynamics. On the basis of modeling and calculating electronic coupling as a function of the angle between the ethynyltetracenes, we suggest that the rotation of ethynyltetracenes to a perpendicular orientation facilitates the formation of independent triplets (i.e., productive singlet fission). To study the role of the linker in facilitating singlet fission between the tetracenes, we have also synthesized the *para*-bis(ethynyltetracenyl)benzene dimers *p*-BETB-ehex and *p*-BETB-ohex (Scheme 1) with different linker units and observe that singlet fission is faster in *p*-BETB-ohex.



Scheme 1: The synthetic scheme for *m*-, *p*-BETB-ohex and *p*-BETB-ehex. (i) NBS, DMF, CH₂Cl₂, 40°C; (ii) Pd(PPh₃)₄, CuI, THF, Et₃N, 60°C.

Table 1. Electrochemical properties of the four dimers compared to the monomer, and the optical gaps of these molecules. The ferrocene/ferrocene redox couple in dichloromethane was used as an internal standard for electrochemical measurements.

Molecule	1 st Oxidation (V)	2 nd Oxidation (V)	$\Delta E(O_{X_2}-O_{X_1})$ (V)	E_{redox} (eV)	$E_{optical}$ (eV)	$E_{optical}-E_{redox}$ (eV)
PET	0.46	---	---	2.38	2.42	0.04
<i>o</i> -BETB	0.37	0.59	0.22	2.32	2.37	0.05
<i>m</i> -BETB	0.41	0.48	0.07	2.30	2.40	0.10
<i>p</i> -BETB-ehex	0.46	0.59	0.13	2.38	2.34	-0.04
<i>p</i> -BETB-ohex	0.33	0.55	0.22	2.21	2.28	0.07

SYNTHETIC AND SPECTROSCOPIC METHODS

The *meta* and the *para* dimers were synthesized as shown in Scheme 1. The alkynyl motif in these dimers allows them to be constructed via the highly efficient Sonogashira reaction.⁶⁶ *m*-BETB was constructed from 5-bromotetracene and the commercially available *meta*-diethynylbenzene. The *para* dimers were synthesized by Sonogashira reaction between the appropriate diethynylbenzene linker unit and 5-bromotetracene. The synthetic details and characterization data are available in the Supporting Information (SI). Broadband femtosecond and nanosecond transient absorption spectra and time-correlated single photon counting traces were collected from solutions of the ethynyltetracene dimers made in 1 mm path length quartz cuvettes using freshly distilled, de-aerated THF. Briefly, the broadband femtosecond TA setup consists of a Coherent Legend amplifier pumping a Spectra Physics OPA to provide the pump beam and a CaF₂ crystal to provide the white light super continuum probe beam. Nanosecond transient absorption spectroscopy was performed using the same probe beam and pump beam from a Alphas Pulselas nanosecond laser. More details on steady state and transient absorption spectroscopy, fluorescence lifetime measurements, and electrochemistry are provided in the SI.

RESULTS AND DISCUSSION

Electrochemistry

The extent to which the ethynyltetracene units are conjugated in *ortho*-, *meta*- and *para*-bis(ethynyltetracenyl)benzene dimers can be estimated from cyclic voltametry (CV). In the dimer the first oxidation should be localized on one of the tetracenes and the second oxidation should take place on the second tetracene. Conjugation between the ethynyltetracenes in a dimer should give rise to a significant difference between the first and second oxidation potentials, because the two ethynyltetracene units are not acting independently. Conversely, if the ethynyltetracene units do not interact, both units in a dimer would oxidize at the same potential and the difference between the first and second oxidation potentials would be close to zero. The cyclic voltammograms of the *ortho*-, *meta*-, and *para*-bis(ethynyltetracenyl)benzene dimers, as well as phenylethynyltetracene (PET, monomer) were collected in dichloromethane, with ferrocene as the internal standard (additional experimental details in SI). We observed two oxidation peaks in all dimers; however, the peaks were poorly resolved in *m*-BETB, due to their proximity (see SI). The oxidation potentials and the values of the splitting between the oxidation peaks are given in Table 1. Based on the magnitude of the splitting of the oxidation potentials, the chromophores that are the most strongly conjugated are *o*-BETB and *p*-BETB-ohex, with $\Delta E(O_{X_2}-O_{X_1})$ values of 0.22 V, *m*-BETB at 0.07

V is the least conjugated and *p*-BETB-ehex is intermediate with a difference of 0.13 V between the two oxidations. The electrochemical properties of the dimers also provide information about the energetics of intramolecular charge resonance (CR) states, which are important in the singlet fission mechanism.^{49, 67} The approximate energy of the intramolecular CR state (E_{redox} , Table 1) can be roughly estimated from the difference between the oxidation (E_{ox}) and the reduction (E_{red}) potentials and a Coulombic term.⁶⁸ The values of E_{ox} , E_{red} , and the electrochemical energy gap for the dimers and the monomer obtained by CV are given in Table S1 in the supporting information. The values of the first excited state ($E_{optical}$), estimated from the absorption spectra of these dimers, are also supplied in Table 1 for comparison. In all molecules the electrochemical gap is energetically comparable to the optical gap, suggesting that CR configurations lie close enough in energy to the locally excited ones to potentially influence singlet fission kinetics, as suggested in the case of the series of TIPS-pentacene dimers.^{37, 69}

Steady state spectra

The intensities and line shapes of the steady-state extinction spectra are representative of the magnitude of the transition dipole moments in the molecules and can reflect the extent of the $S_1S_0-S_0S_1$ coupling between the chromophores within the dimers. In our previous work, we showed that the ethynyltetracene moieties in *o*-BETB are aligned such that the transition dipole moments of the lower energy transition (along the short axis of the acene) are coupled in an H-aggregate-like manner, as evidenced by the enhanced ν_{0-1} and diminished ν_{0-0} absorption compared to PET (Figure 2).⁴⁹ The absorption of the *ortho* dimer is redistributed to longer wavelengths, but the integrated intensity in the visible region is less than twice that of the monomer. The absorption spectrum of *m*-BETB is nearly identical to that of PET, but with a small red-shift of 4 nm (0.02 eV). The relative intensities of the ν_{0-0} and the ν_{0-1} vibronic features of the PET and the *m*-BETB are identical. The most notable

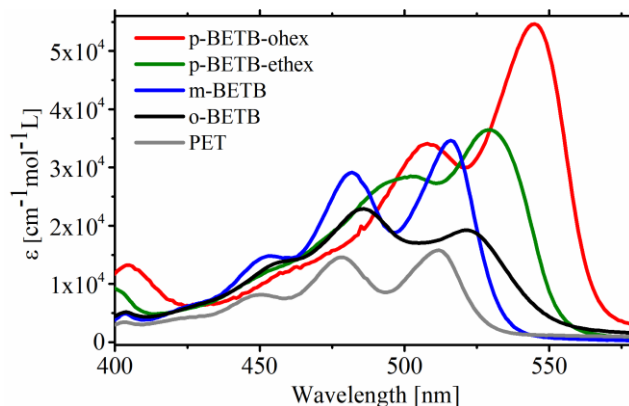
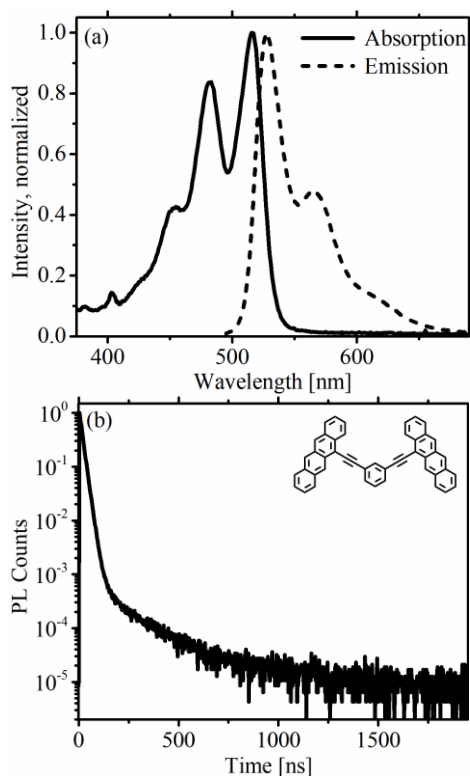


Figure 2. The extinction spectra of *m*-BETB, *p*-BETB-ehex, and *p*-BETB-ohex compared to *o*-BETB and PET in THF solution.

1 difference between PET and *m*-BETB absorption properties is in
 2 their molar absorptivity spectra: the molar absorptivity of *m*-BETB
 3 is twice that of PET in the visible part of the spectrum (the ratio of
 4 integrated areas is 2.0). This suggests that tetracenes in *m*-BETB are
 5 effectively independent of each other and the electronic coupling between
 6 them is weak.

7 The absorption properties of the *p*-BETB-ohex and *p*-BETB-ehex
 8 are different from those of *o*-BETB, *m*-BETB and the monomer
 9 PET. The molar absorptivity of *p*-BETB-ehex in the visible region is
 10 more than twice that of PET, with the area under the curve greater
 11 than twice that of PET by a factor of 2.6). The red shift and significant
 12 difference between the integrated absorptivity of the dimer versus
 13 twice that of the monomer suggest strong exciton coupling between
 14 the two ethynyltetracene units in *p*-BETB-ehex.^{70,71} The increase
 15 in molar absorptivity of *p*-BETB-ohex over PET is even greater,
 16 with *p*-BETB-ohex having an absorptivity more than three times
 17 greater than that of PET in the visible region (the ratio of the
 18 integrated areas of the absorption bands is 3.3), and is accompanied
 19 by a substantial red-shift in the visible absorption. This further
 20 demonstrates that the electron-donating alkoxy substituents on the
 21 bridging benzene ring significantly alter the electronic structure of
 22 the dimers and in this case appear to enhance exciton coupling. The
 23 intensity of the emission (see SI) gives insight into the rates of the
 24 excited-state decay channels. Analogously to *o*-BETB, the *para* dimers
 25 are very weakly emissive ($\Phi_f < 1\%$), suggesting that the process
 26 which quenches the fluorescence in these systems is orders of mag-
 27 nitude faster than ~ 10 ns (viz. the excited state lifetime of the

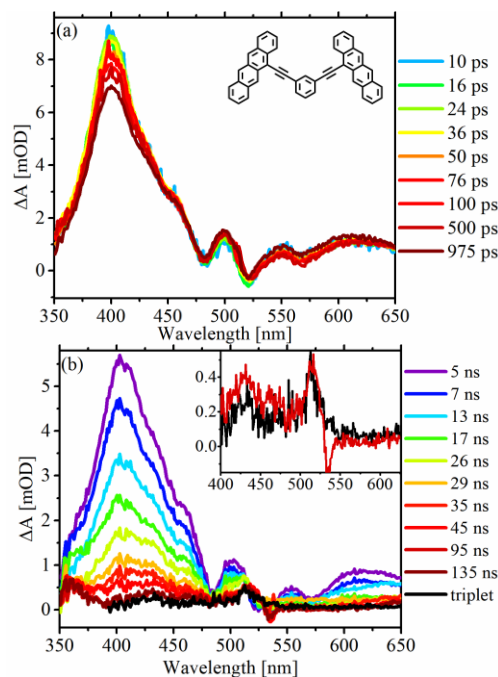


27 **Figure 3.** (a) Steady state absorption and emission of *m*-BETB in THF.
 28 (b) Emission decay of *m*-BETB in THF (excitation at 405 nm, emission
 29 at 570 nm), with noticeable delayed fluorescence on the ~ 200 ns time-
 30 scale.

31 monomer PET, see SI). The analogous *para*-bis(ethynylanthra-
 32 crenyl)benzene dimers emit with high quantum efficiencies: 97% for
 33 *para*-bis(ethynylanthracenyl)benzene,⁵² and 60 % for the analogous
 34 hexyloxy substituted *para*-bis(ethynylanthracenyl)benzene.⁷² Similar-
 35 ly to the comparison of *o*-BETB to its anthracene analog in our
 36 previous work, the high quantum efficiency of emission of the an-
 37 thracene dimers compared to the tetracene dimers suggests that a
 38 rapid excited-state decay channel is available in the *para*-tetracene
 39 dimers, which is not available in the anthracene analogs. Conversely,
 40 *m*-BETB is strongly emissive in solution (Figure 3), with a quantum
 41 yield of 62%, suggesting that the rate and yield of non-radiative ex-
 42 cited-state decay processes are not significant in this system. The
 43 emission decay, shown in Figure 3b, has a small delayed component
 44 (~ 190 ns), analogous to those observed for weakly-coupled tetra-
 45 cene dimers by Bardeen⁷³ and Damrauer⁷⁴, and could be sugges-
 46 tive of triplet-triplet recombination. Presuming that the delayed fluo-
 47 rescence is a result of recombination of two geminate triplets gener-
 48 ated by singlet fission, we used a kinetic model analogous to the
 49 one reported by Muller *et al.* and Cook *et al.* to estimate the yield of
 50 singlet fission to be approximately 1% in *m*-BETB, and the rate of the
 51 decay of the delayed fluorescence to be solvent dependent (de-
 52 tails in SI). The photoluminescence lifetimes of all solutions of *m*-
 53 BETB in THF with concentrations varying from 1.5 μ M to 21 μ M
 54 (see SI for details) is the same (~ 170 ns), indicating the absence of
 55 any intermolecular reactions between two dimers in solution. The
 56 triplets on *m*-BETB therefore recombine via a geminate pathway.

57 Transient absorption of *m*-BETB

58 The femtosecond transient absorption spectra of *m*-BETB in THF
 59 following excitation at 515 nm are shown in Figure 4(a). The char-
 60 acteristic acene $S_n \leftarrow S_1$ absorption peak is observed at 400 nm,



61 **Figure 4.** The (a) femtosecond and (b) nanosecond transient absorp-
 62 tion of *m*-BETB, with the sensitized $T_n \leftarrow T_1$ absorption shown in
 63 black. Inset to b) shows an overlay of the transient spectrum of
 64 *m*-BETB at 135 ns and the sensitized $T_n \leftarrow T_1$ spectrum.

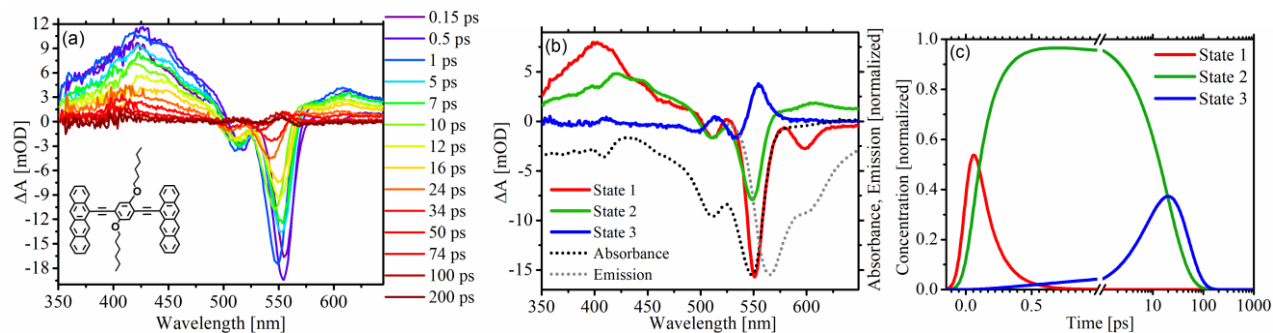


Figure 5. The femtosecond transient absorption (a), the species associated difference spectra (b) and concentration curves (c) from the target analysis of the TA data of *p*-BETB-ohex in THF.

along with ground state bleach at 516 nm and 480 nm – similar features were observed in the case of the ethynyltetracene monomer (ETTMS) in our earlier studies.⁴⁹ Between 10 ps and 975 ps, there is no significant evolution of these spectral features. The $S_n \leftarrow S_1$ absorption decays after 5 ns when excited at 532 nm in a nanosecond pump broadband transient absorption experiment (Figure 4b), with a concomitant rise of a positive feature at \sim 510 nm. A peak in this spectral region has been previously observed for $T_n \leftarrow T_1$ absorption in acenes like 5,12-diphenyltetracene (DPT) and ET-TMS.^{37, 49, 75} More importantly, the spectral shape at 135 ns is identical to the sensitized $T_n \leftarrow T_1$ absorption of *m*-BETB (inset to Figure 4b). The rise of the absorption feature at 510 nm is slow, suggesting that the triplets could be generated in this system by intersystem crossing, with the rates similar to other tetracene derivatives.⁷⁶ The transient absorption data was fit with a two-state sequential model (see SI) with a time constant of 15 ns for the rise of the triplet feature and a triplet lifetime of 4.6 μ s. The triplets could also arise from a channel in which very slow (and therefore inefficient) singlet fission results in the delayed fluorescence from *m*-BETB in solution (\sim 190 ns, Figure 3b).

It is reasonable to assign the negligible singlet fission and slow formation of triplets in *m*-BETB in solution to the weak non-adiabatic coupling, similar to the *meta* dimer in a series of tetracene dimers reported by Muller et al.⁴⁰ *Ab initio* calculations further support this notion. The coupling parameter, $|\gamma|^2$, between the S_1 and the $^1(T_1T_1)$ states in *m*-BETB is calculated to be 4.6×10^{-5} , a value that is about three orders of magnitude smaller than for *o*-BETB (0.04).⁶⁴ Additionally, the computed binding energy (E_b) of the triplets (calculated as the difference between the energy of the biexciton state and the two separated triplets) indicates how strongly the T_1 excitons are coupled in the $^1(T_1T_1)$ state within the dimer and is reflective of the intra-molecular chromophore coupling. The value of E_b in *m*-BETB was calculated to be <0.001 eV (compared to 0.15 eV for *o*-BETB), suggesting that the tetracenes are weakly coupled in this dimer. Although singlet fission was observed to proceed on a 200 ps timescale in the TIPS-pentacene analog of *m*-BETB, the rate of singlet fission reported in the *meta* dimer in the series of the TIPS-pentacene dimers was slower by at least three orders of magnitude compared to the *ortho* and *para* dimers.^{37, 77}

Transient absorption of *p*-BETB-ohex and *p*-BETB-ehex in THF

The TA spectra of *p*-BETB-ohex and *p*-BETB-ehex in THF, excited at 545 nm, and 530 nm, respectively, are shown in Figure 5(a) and 6(a). At early times (< 25 ps), both compounds display the characteristic excited-state absorption band at 425 nm, and ground-state bleach at 520-540 nm. The vibronic structure associated with

ground-state absorption and excited-state emission (through contributions from ground-state bleaching and stimulated emission) are superimposed on the broader excited-state absorption bands in the overall transient absorption spectra as seen in Figures 5(b) and 6(b). The broad absorption feature at 425 nm decays within 100 ps, giving rise to an induced absorption peak at 555 nm in *p*-BETB-ohex and 540 nm in *p*-BETB-ehex. This feature of the *para* dimers decays much more rapidly than that of *m*-BETB, and most importantly the spectral shape of the induced absorption of *p*-BETB-ehex and *p*-BETB-ohex at \sim 100 ps is also different from that of *o*-BETB reported previously.⁴⁹

To get an idea of the excited-state dynamics in the *p*-BETB dimers, we subjected the TA data to target analysis.⁷⁸ We obtained the best fit using a 3-state sequential model ($[state\ 1] \rightarrow [state\ 2] \rightarrow [state\ 3]$). The species associated difference spectra (SADS) and corresponding concentration curves obtained from target analysis are shown in Figures 5 and 6, respectively. The shapes of the SADS of *p*-BETB-ohex and *p*-BETB-ehex in THF are qualitatively similar (Figure 5(b) and 6(b)). The spectral signature of state 1 in both systems resembles the typical acene $S_n \leftarrow S_1$ absorption⁴⁹, with a sharp peak in the 375-470 nm region with a larger (negative) amplitude from ground-state bleach and stimulated emission. In both systems, state 1 rapidly decays to state 2 with a broader band in the 375-470 nm region, a net absorption from 575 – 650 nm and similar ground state bleach features to state 1. The spectral shape of state 2 of *p*-BETB-ohex and *p*-BETB-ehex in THF resembles that of the $^1(T_1T_1)$ state absorption in *o*-BETB. The difference in the SADS corresponding to state 2 in *p*-BETB-ohex and *p*-BETB-ehex suggests that the spectrum originating from this state is dependent upon the structure of the bridging linker, and therefore the coupling between acenes. Recall that based on the splitting in the oxidation potential peaks, the conjugation between the tetracenes is the strongest in *o*-BETB and *p*-BETB-ohex (0.22 V), and significantly weaker (0.13 V) in *p*-BETB-ehex. The rate of formation of state 2 in the *para* dimers, however, is much faster than the formation of $^1(T_1T_1)$ in *o*-BETB. The target analysis gives values of 0.1 ps (essentially on the timescale of the instrument response) for *p*-BETB-ohex and 0.4 ps for *p*-BETB-ehex (Table 2), while in *o*-BETB, $^1(T_1T_1)$ was formed in 2 ps. The faster rate of formation in the *para* dimers than in the *ortho* dimer highlights the importance of through-bond coupling. The result suggests that through-bond coupling in the planar *p*-BETB-ehex is stronger than the coupling in *o*-BETB, in which the chromophores are predominantly coupled through-space, but also exhibit some through-bond coupling via the linker, albeit to a lesser extent because the chromophores in *o*-BETB are not in plane with

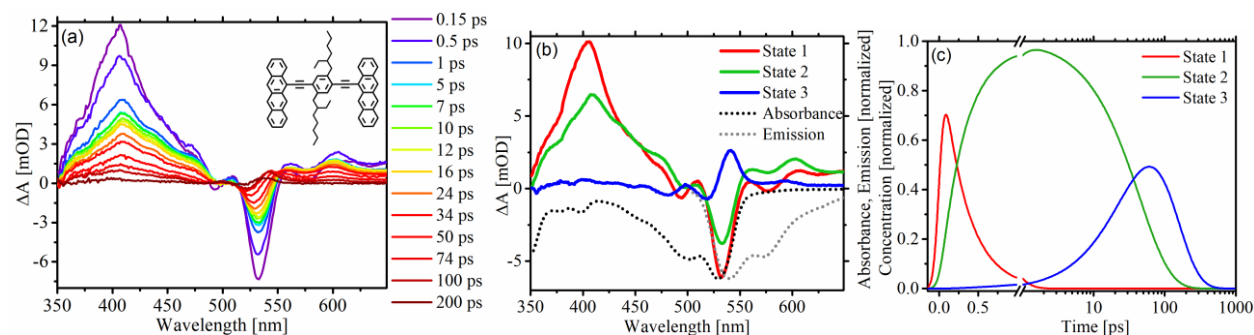


Figure 6. The femtosecond transient absorption (a), the species associated difference spectra (b) and concentration curves (c) from the target analysis of the TA data of *p*-BETB-ehex in THF.

the linker. Unlike in *o*-BETB, the $^1(T_1T_1)$ state in *p*-BETB-ohex and *p*-BETB-ehex decays to a third state with an identifiably different spectral signature, with prominent induced absorption peaks at 555 nm and 540 nm in *p*-BETB-ohex and *p*-BETB-ehex, respectively. The spectral shape of state 3 in *p*-BETB-ohex and *p*-BETB-ehex in solution bears a strong resemblance to that of the sensitized $T_n \leftarrow T_1$ induced absorption of the monomer, ET-TMS.⁴⁹

The absorption of state 3 could correspond to either one or two triplets per dimer. There are two factors which suggest that state 3 corresponds to absorption of two triplets on the same dimer: (i) the rate of formation of state 3 is fast – 19 ps in *p*-BETB-ohex and 48 ps in *p*-BETB-ehex (Table 2). These rates of T_1 formation are too fast for intersystem crossing in acenes⁷⁶, but are in the range of the measured singlet fission rates in tetracene,^{8,37,79,80}. (ii) The rate of the decay of state 3 is very fast – 20 ps in *p*-BETB-ohex and 76 ps in *p*-BETB-ehex. Typically, a single triplet exciton localized on an acene dimer decays on the timescale of microseconds.⁷⁶ However, the recent studies of pentacene dimers showed that when two triplet excitons are located on the same dimer, the $T_n \leftarrow T_1$ absorption decays on the 10-100 ps timescale, due to the favorable T_1 - T_1 fusion pathway to the ground state.^{77,81} Therefore, the SADS for state 3 in the *para* dimers in THF is the spectral signature of two triplets in close proximity to each other. The most likely origin of these two triplets is via singlet fission.

In Figure 7, an overlay of the SADS for state 3 of *p*-BETB-ehex is made with $T_n \leftarrow T_1$ absorption spectra for a single triplet sensitized onto *p*-BETB-ehex and triplet sensitized onto the model monomer compound, ET-TMS. The details regarding sensitization experiments have been previously reported.⁴⁹ For both the sensitized spectra, a spectral shift is required to line up the peaks with the state 3 SADS. Despite small discrepancies in the intensities in the 400 - 500 nm region, the relative peak positions and relative intensities overlay well, strongly suggesting that state 3 corresponds to $T_n \leftarrow T_1$ induced absorption in *p*-BETB-ehex. It is worth noting that

Table 2. The time constants (in ps) of the decays used to fit the TA data of the dimers in THF.

	<i>o</i> -BETB ¹	<i>m</i> -BETB ²	<i>p</i> -BETB -ohex	<i>p</i> -BETB -ehex
$\tau [S_1 \rightarrow ^1(T_1T_1)]$	2.0	1.5×10^4	0.1	0.4
$\tau [^1(T_1T_1) \rightarrow ^3T_1]$	-	-	19	48
$\tau [^3T_1]$	-	4.6×10^6	20	76

¹Taken from previously published work, reference 17.

²Time constants corresponding to the intersystem crossing rate and the decay of that triplet.

state 3 resembles the $T_n \leftarrow T_1$ induced absorption of the monomer more closely than that of the dimer. We surmise that in the case of the sensitized triplet on the dimer the $T_n \leftarrow T_1$ excitation maybe delocalized over more than just the one ethynyltetracene unit on to the phenyl linker or even the second ethynyltetracene. Therefore the sensitized triplet absorption of the dimer differs from that of the monomer ET-TMS. Whereas when singlet fission produces two triplet excitons in the dimer they likely localize to their respective acenes; and when the acenes rotate out of plane from each other the spectrum of the triplet excitons effectively resemble the sensitized triplet spectrum of monomer ET-TMS.⁴⁹ We estimated the triplet yield in these compounds by scaling the target analysis populations by the extinction coefficients of the singlet and the triplet absorptions (see S.I. for details) and obtained 94% for *p*-BETB-ehex and 70% for *p*-BETB-ohex. The triplet yields are low in these *para* dimers because the rate of recombination of the triplets is fast relative to the rate of their formation.

Surprisingly, the observed behavior of our *ortho*-,⁴⁹ *meta*- and *para*-ethynyltetracene dimers is different from that of isomorphous dimers of TIPS-pentacene reported by Tykwinski, Guldi and coworkers.³⁷ All TIPS-pentacene dimers undergo singlet fission, with only the *meta*-TIPS-pentacene dimer undergoing fission slowly enough to be resolved by the instrument.^{45,82,83} In our previous work on *o*-BETB, the formation of only the biexciton state was observed whereas here

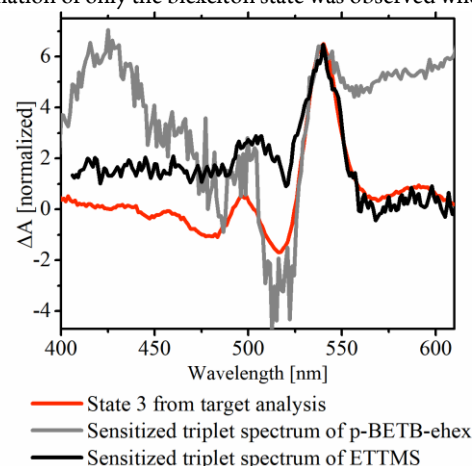


Figure 7. The plot shows the spectral signature of state 3 from target analysis of *p*-BETB-ehex in THF compared to the normalized sensitized $T_n \leftarrow T_1$ absorption of ET-TMS (red-shifted, 20 nm) and sensitized $T_n \leftarrow T_1$ absorption of *p*-BETB-ehex in THF (blue-shifted, 9 nm).

we find evidence of predominantly radiative decay in *m*-BETB. We observe that the *para*-ethynyltetracene dimer forms two independent triplet states via the biexciton state. Using TCSPC (with more dynamic range), we observe that a small fraction (1%, see SI) of *m*-BETB molecules gives rise to delayed fluorescence, which were not captured in transient absorption. The delayed fluorescence in *m*-BETB is solvent dependent, which is similar to the *meta*-TIPS-pentacene dimer. Solvent dependence suggests involvement of charge resonance configurations. However, in contrast to *meta*-TIPS-pentacene⁸⁴, we do not observe the spectral signatures of the charge resonance states in the transient absorption spectra of *m*-BETB. We explain this difference by noting that the optical and electrochemical gaps are closer in *meta*-TIPS-pentacene than in *m*-BETB (1.88 eV vs 1.87 eV in the former and 2.30 eV versus 2.40 eV in the latter), which suggests that there is a smaller contribution of the charge resonance states in *m*-BETB. The analysis of the S_1 wave-function shows 0.2% of charge resonance configurations in *m*-BETB. In the TIPS-pentacene dimers, the energy of $2 \times E(T_1)$ at 1.54 eV is far below the energy of the S_1 state at 1.88 eV. This energetic driving force for singlet fission in the TIPS-pentacene systems results in ultrafast kinetics from which mechanistic information is not easily obtained. In the case of ethynyltetracene dimers presented here, the $E(S_1) \approx 2E(T_1)$ isoenergetic conditions make singlet fission only slightly favorable. As a result of which the subtle differences in the effect of through-bond and through space coupling can be investigated.

The *ortho*- and the *para*- bis-ethynylbenzene dimers exhibit distinctly different excited-state dynamics. The S_1 state in the *para* dimers yield the $^1(T_1T_1)$ state, which decays to form independent triplets, whereas the $^1(T_1T_1)$ state in *o*-BETB relaxes to the ground state without producing independent triplet excitons. According to the model proposed by Abraham and Mayhall (AM model), both *ortho* and *para* dimers should produce bound $^1(T_1T_1)$ states that are unlikely to form non-interacting triplet excitons.⁶⁵ Although the AM model correctly captures the important aspect of the nature of the biexciton states in these systems (as compared against RAS-2SF-CI calculations) and explains the observations for *o*-BETB, it does not explain the observed singlet fission dynamics in our *para* dimers, which we attribute to its static nature. The difference in the excited-state processes in the *ortho* and *para* dimers and the deviation from the AM model can be rationalized by considering rotational motions of the chromophores in these dimers. In *o*-BETB the tetracenes can rotate, they always retain some degree of π overlap, which results in non-zero biexciton binding energy. In the *para* dimers, on the other hand, the chromophore interaction is limited to through-bond only. Upon twisting of one of the tetracenes perpendicular to the plane of the rest of the molecule, the electronic coupling between the chromophores is broken and E_b becomes zero (Table 3). Consequently, the triplets from the correlated triplet pair state become in

Table 3. The RAS-2SF-CI computed excited state energies (in eV) and, binding energy (in eV) and coupling for *p*-BETB-ehex the *para* dimer as a function of the dihedral angle (in degrees) between the tetracenes.

Angle	$E(S_1)$	$E(^1(T_1T_1))$	E_b	$ \gamma ^2$
0	3.84	3.38	0.04	0.020
30	3.91	3.45	0.04	0.020
60	3.86	3.37	0.01	0.004
90	3.87	3.39	0.00	0.000

dependent of each other. Thus, in order to explain singlet-fission trends in flexible dimers, the AM model needs to be extended to account for changes in electronic structure upon twisting. Figure 8 shows the possible molecular orientations corresponding to the correlated and independent triplet pair states in *p*-BETB-ehex. Further insight into the effect of rotation on the excited-state energies of *p*-BETB-ehex can be obtained from theory. The energies of the S_1 , $^1(T_1T_1)$, and $^5(T_1T_1)$ states were computed as a function of the dihedral angle between the tetracenes in *p*-BETB-ehex using the restricted active space configuration interaction with double spin-flip method (RAS-2SF-CI, Table 3). The minimum of the S_1 potential energy surface corresponds to a planar geometry and the $^1(T_1T_1)$, and $^5(T_1T_1)$ states are energetically downhill from the S_1 state by about 0.4 eV at all rotational angles. The coupling between the S_1 and the $^1(T_1T_1)$ states ($||\gamma||^2$) was calculated to be largest at a planar geometry (0.020), and is 0.004 at 60° and drops to 0.000 at 90°. The $^1(T_1T_1)$ surface has a minimum at 60 degrees, while the $^5(T_1T_1)$ surface has a minimum at 90 degrees, at which the $^1(T_1T_1)$ and the $^5(T_1T_1)$ states become degenerate (see Table 3). These values indicate that the triplet excitons from the correlated triplet pair state in *p*-BETB-ehex can become non-interacting in the $^5(T_1T_1)$ state when the tetracenes rotate perpendicular to each other within the dimer.

Transient absorption of *p*-BETB-ehex in PMMA

If rotational motion of the tetracene in *para* dimer in solution provides the mechanism for generating free triplets, then restricting that motion should reduce the rate and the yield of the formation of free triplets. To test this hypothesis, a solution of *p*-BETB-ehex in a rigid polymer matrix, poly(methylmethacrylate) (PMMA) was prepared. *p*-BETB-ehex in PMMA produces a substantial amount of emission at room temperature, with a quantum efficiency of ~10% (see SI), which means that a significant fraction of the molecules are confined to a geometry in which the radiative decay is the predominant relaxation pathway from the singlet excited state. From a comparison of the transient absorption spectra of *p*-BETB-ehex in THF and in PMMA (Figure 9), it is evident that in PMMA the excited state absorption corresponding to $S_1 \rightarrow S_n$ absorption centered at 420 nm decays much more slowly. The characteristic $T_n \leftarrow T_1$ absorption peak at 550 nm still forms in this media; however, the rate of its formation is much slower than for *p*-BETB-ehex in THF. Unlike *p*-BETB-ehex in THF, the transient signals observed from *p*-BETB-ehex in PMMA cannot be fit using a 3-state sequential model. PMMA, which a more rigid medium than THF, raises the barrier to rotation for the tetracene units in *p*-BETB-ehex along the diethynylbenzene linker. This results in *p*-BETB-ehex dimers that are conformationally locked in the polymer matrix in a distribution of rotational angles. Upon excitation in this rigid medium not all the *p*-BETB-ehex molecules which end up in the $^1(T_1T_1)$ state will be able to rotate and form independent triplets. The TA spectra from

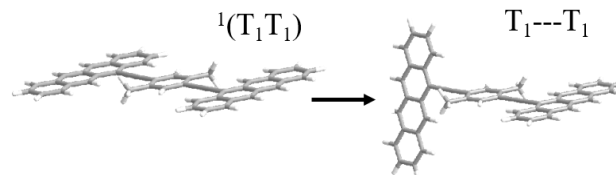


Figure 8. The proposed decoupling of the correlated triplet state in *p*-BETB-ehex (alkyl chains have been removed for clarity) to give rise to two independent triplets.

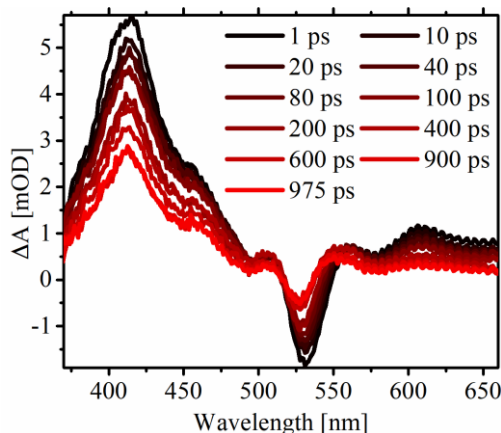


Figure 9. The femtosecond transient absorption of *p*-BETB-ehex in PMMA.

p-BETB-ehex in PMMA with the tetracene units locked in all dihedral angles can be modeled as a sum of signals from two model populations with extreme conformations of the *para* dimer: *population 1* with the tetracenes coplanar with each other and *population 2* with tetracenes perpendicular (Figure 10). *Population 1* represents the dimer molecules in PMMA which cannot undergo singlet fission completely, and the $^1(T_1T_1)$ remains in equilibrium with the S_1 state, giving rise to the fluorescence signal from the PMMA sample. *Population 2* is representative of dimer molecules that can fully undergo singlet fission to two independent triplets, and gives rise to the triplet band at 550 nm in the TA spectra at 957 ns. Using compartmental models to represent the excited-state processes in the distinct populations, it is possible to obtain concentration curves that describe the dynamics of the excited states (details in the SI).⁷⁸ The transient absorption spectra corresponding to both model populations *1* and *2* can be derived by multiplying the concentration curves with the Species Associated Difference Spectra (from Figure 6b) corresponding to the S_1 , $^1(T_1T_1)$, and T_1 - T_1 states (see SI). The fractions of the model *population 1* and *population 2* that best represent *p*-BETB-ehex in PMMA is obtained by comparing the time slice of the transient absorption data at 425 nm with the time slices at the same wavelength of the modeled transient absorption data; the latter is obtained by combining the TA spectra of the *population 1* and *population 2* in different fractions and optimizing the time constants for the various excited state processes by repeated iterations in MATLAB. As seen in Figure 11, the best representation of the excited state dynamics is obtained by combining the dynamics of populations *1* and *2* in equal fractions and reproduces the 10% quantum yield measured from the PMMA film. This suggests that in a more

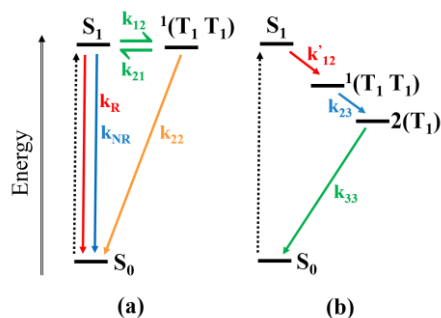


Figure 10. The state diagrams showing (a) population 1 and (b) population 2 used to model the TA data from *p*-BETB-ehex in PMMA.

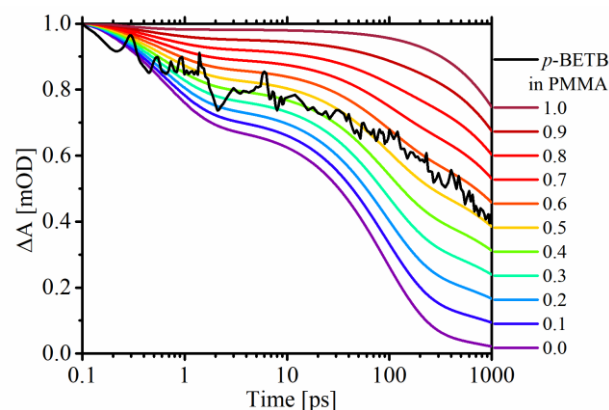


Figure 11. Dynamics of excited state absorption at 425 nm of *p*-BETB-ehex in PMMA (black trace) overlaid with the time slices at 425 nm of transient absorption spectra obtained by combining modelled transient absorption of *population 1* and *population 2* in different fractions. Numbers in the legend show the fraction of *population 1* in that model. The rate constants (s^{-1}) that gave the best fit are: $k_r = 5.5 \times 10^7$, $k_{nr} = 2.9 \times 10^6$, $k_{12} = 5 \times 10^{11}$, $k_{21} = 4 \times 10^{12}$, $k_{22} = 2 \times 10^9$, $k_{12}' = 1.6 \times 10^{12}$, $k_{23} = 1.2 \times 10^{10}$, $k_{33} = 1.2 \times 10^9$.

realistic model, the tetracene units in *p*-BETB-ehex in the polymer matrix would be locked at all dihedral angles with equal probability. This is quite likely the case since the monomer units in PMMA are small, and would not hold the tetracenes at any one angle preferentially by non-covalent interactions. The TA spectra of *p*-BETB-ehex in PMMA and its modeling using conformationally restricted populations emphasizes the importance of the rotation of the tetracene units in allowing the $^1(T_1T_1)$ state to separate to independent triplets in *p*-BETB-ehex and not in *o*-BETB – despite the similarities in electronic coupling. A similar rotational mechanism of formation of triplets from the correlated triplet pair state has been reported in bipentacene dimers by Tayebjee et al.⁹⁰ The phenylene bridges in these dimers resulted in a long lived $^5(T_1T_1)$ state that had a lifetime >200 ns and allowed the authors to characterize the quintet state using time-resolved EPR. According to the authors, the coupling in the bipentacene BP2 with the pentacenes separated by two phenylene units is greater than in BP3 with the pentacenes separated by three phenylene units. This difference is reflected in the fact that in BP3 the quintet state evolves in to dissociated triplets while in BP2 the quintet state gives rise to triplets that are still weakly interacting. Although an analogous analysis for our *p*-BETB systems would be insightful, it is unlikely to be fruitful in the case of our dimers. Based on the fast timescale (< 100 ps) of the conversion from $^1(T_1T_1)$ to electronically independent triplets ($2 \times T_1$) in *p*-BETB dimers, followed by rapid return to the ground state, we can expect that the triplet excitons do not have enough time to undergo spin dephasing, and only undergo electronic decoupling. Analogous ESR experiments to those carried out by Tayebjee et al. would be hampered by the short excited state lifetime observed in *p*-BETB dimers.

Finally, of additional interest are the differences in the excited-state kinetics of *p*-BETB-ohex and *p*-BETB-ehex. All three of the processes: relaxation of S_1 into $^1(T_1T_1)$, conversion of $^1(T_1T_1)$ to independent triplets, and the decay of the resultant triplets are faster in *p*-BETB-ohex compared to *p*-BETB-ehex (Table 2). The difference in the coupling of the tetracene units in *p*-BETB-ohex and

p-BETB-ehex can be understood in terms of the relative orbital energies of the tetracenes and the two bis(ethynyl)benzene linkers. A qualitative diagram showing the relative orbital energies of these molecules is provided in Figure 12. In the alkyl-substituted benzene linker, the orbitals are expected to lie energetically far from those of the tetracenes and the coupling is not expected to be very large. However, introducing the electron donating hexyloxy substituents onto the benzene linker raises the energy of the HOMO, and therefore brings the orbital energies of the linker closer to those of the tetracenes, resulting in stronger coupling between the acenes and faster singlet fission in *p*-BETB-ohex.

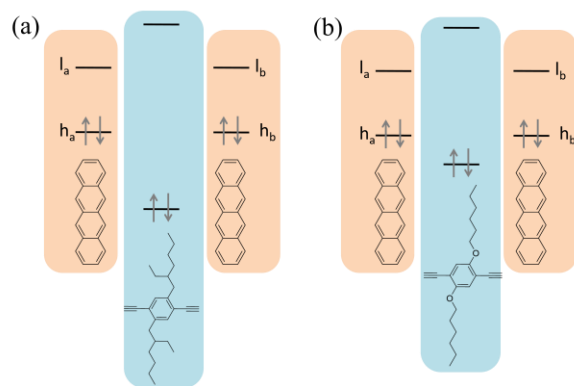


Figure 12. A diagram showing the closer lying orbitals of the linker and the tetracenes in (a) *p*-BETB-ehex compared to (b) *p*-BETB-ohex. l_a/b and h_a/b are the frontier molecular orbitals of tetracene.

CONCLUSIONS

We have synthesized the *meta* and *para* analogues of the previously reported *ortho*-bis(ethynyltetracene)benzene to study the role of through-bond vs. through-space coupling in facilitating singlet fission between the tetracene units. The *ortho*- and *para*-ethynylbenzene linkers provide conjugation between the tetracene units while the *meta*-ethynylbenzene linker is cross-conjugating in the ground state. Using broadband femtosecond transient absorption spectroscopy, we have established that the *meta*-(ethynyltetracene)benzene predominantly undergoes radiative decay in the excited state. Surprisingly, the *para*-bis(ethynyltetracene)benzene dimer undergoes complete singlet fission, forming independent triplet states via rotation of the acenes out of plane from each other. As reported previously, the *ortho*-bis(ethynyltetracene)benzene dimer only forms the intermediate correlated triplet pair state.

Comparing the behavior of *ortho*-, *meta*- and *para*-bis(ethynyltetracene)benzene dimers provides crucial insight into the role of conjugation and through-bond coupling in singlet fission in dimers. The *ortho* and *para* dimers in which the tetracene units are conjugated through the ethynylbenzene linker exhibit singlet fission while the cross-linked *meta* dimer predominantly undergoes radiative decay. Furthermore the $[S_1] \rightarrow [^1(T_1T_1)]$ process is faster in *p*-BETB-ohex and *p*-BETB-ehex than in *o*-BETB, suggesting that the through-bond coupling operating in the *para* dimers is stronger than the combined through-space and through-bond coupling operating in the *ortho* dimer. Unlike in the case of a series of pentacene dimers, where the energetics are so favorable for singlet fission that the *ortho*-, *meta*- and *para*-TIPS-pentacene dimers all displayed triplet absorption signatures in picosecond timescales, in our case, only the *para* dimer forms independent triplets on similar timescales. This provides an insightful comparison with the *meta* dimer which

does not form a significant number of triplets and the *ortho* dimer which only forms the intermediate correlated triplet pair state. We attribute the difference in the excited-state dynamics of the *ortho* and *para* dimers to the rotational flexibility of the acenes in the *para* dimer, which breaks the coupling between the chromophores and allows the triplets to separate from the correlated triplet pair state. Such rotation of the tetracene units in the *ortho* dimer is hindered because they are confined to a cofacial orientation. The role of tetracenes rotating to form separated triplets is clear when comparing the transient absorption of the *para* dimer in PMMA to that in THF. PMMA being a more rigid medium prevents the rotation and significantly hinders the formation of the two non-interacting triplets.

A comparison of the two *para*-bis(ethynyltetracene)benzene dimers (*p*-BETB-ohex vs. *p*-BETB-ehex) provides insight into the role of the energetics of the linker in singlet fission in covalent dimers. The hexyloxy-bis(ethynyl)benzene linker in *p*-BETB-ohex has molecular orbitals that are closer in energy to orbitals of tetracenes than the 2-ethylhexyl-bis(ethynyl)benzene linker in *p*-BETB-ehex. This results in better mixing of the linker orbitals with those of the tetracenes and thus better coupling in *p*-BETB-ohex than in *p*-BETB-ehex. Better coupling between the tetracene units results in faster formation of the correlated triplet pair state and the separated triplets in *p*-BETB-ohex than in *p*-BETB-ehex – highlighting the role of linker energetics in singlet fission.

In separate experiments reported elsewhere, a comparison of the excited state dynamics of the *meta* and *para* dimers in neat thin films⁹¹ has allowed us to separately probe intra- and inter-dimer singlet fission between tetracene units. While the *meta* dimer doesn't fission in THF solution, in film inter-dimer singlet fission is turned on facilitated by through space interactions between the ethynyltetracene units on adjacent dimers. In films of the *para* dimer, singlet fission was facilitated by both *intra*-dimer through bond coupling, and *inter*-dimer through space coupling such that the depopulation of the singlet state happened at least twice (within the instrument response) as fast compared to THF solution.

ASSOCIATED CONTENT

The synthetic details, structural characterization of the materials, electrochemical data, details of sample preparation for spectroscopy, and excited state kinetic models are provided in the Supporting Information. This material is available free of charge via the Internet at <http://pubs.acs.org>.

AUTHOR INFORMATION

Corresponding Author

*stephen.bradforth@usc.edu

*met@usc.edu

Author Contributions

The manuscript was written through contributions of all authors. All authors have given approval to the final version of the manuscript.

‡N.V.K and J.J. contributed equally.

Present Addresses

† nadia.korovina@nrel.gov, National Renewable Energy Laboratory, 15013 Denver West Pkwy, Golden, Colorado 80401, United States

§xintianf@gmail.com, Department of Chemistry, University of California, Berkeley, California 94720; Q-Chem Inc., 6601 Owens Drive, Suite 105 Pleasanton, California 94588

Funding Sources

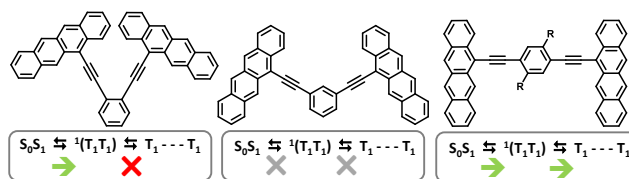
M.E.T., N.V.K., S.E.B and J.J. acknowledge support from the Center for Energy Nanoscience, an Energy Frontier Research Center funded by the U.S., Office of Science, Office of Basic Energy Sciences (DE SC0001013). M.E.T. and N.V.K. additionally were supported by the Nanoflex Power Corporation. A.I.K. acknowledges support through the DE FG02 05ER15685 grant (Department of Energy).

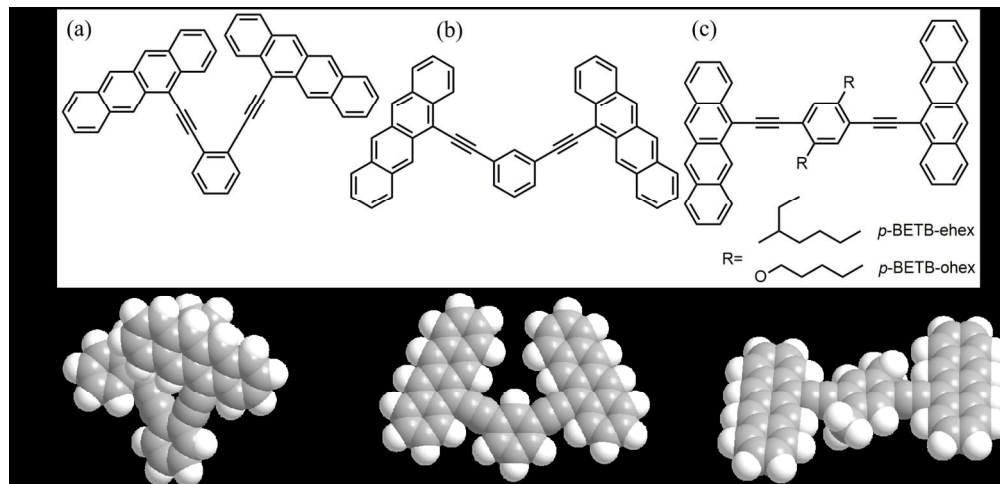
REFERENCES

- Smith, M. B.; Michl, J., Singlet Fission. *Chemical Reviews* **2010**, *110* (11), 6891-6936.
- Piland, G. B.; Burdett, J. J.; Dillon, R. J.; Bardeen, C. J., Singlet Fission: From Coherences to Kinetics. *The Journal of Physical Chemistry Letters* **2014**, *5* (13), 2312-2319.
- Casanova, D., Theoretical Modeling of Singlet Fission. *Chemical Reviews* **2018**.
- Hanna, M. C.; Nozik, A. J., Solar conversion efficiency of photovoltaic and photoelectrolysis cells with carrier multiplication absorbers. *Journal of Applied Physics* **2006**, *100* (7), 074510.
- Tayebjee, M. J. Y.; Gray-Weale, A. A.; Schmidt, T. W., Thermodynamic Limit of Exciton Fission Solar Cell Efficiency. *The Journal of Physical Chemistry Letters* **2012**, *3* (19), 2749-2754.
- Congreve, D. N.; Lee, J.; Thompson, N. J.; Hontz, E.; Yost, S. R.; Reuswig, P. D.; Bahlke, M. E.; Reineke, S.; Van Voorhis, T.; Baldo, M. A., External Quantum Efficiency Above 100% in a Singlet-Exciton-Fission-Based Organic Photovoltaic Cell. *Science* **2013**, *340* (6130), 334-337.
- Schrauben, J. N.; Zhao, Y.; Mercado, C.; Dron, P. I.; Ryerson, J. L.; Michl, J.; Zhu, K.; Johnson, J. C., Photocurrent Enhanced by Singlet Fission in a Dye-Sensitized Solar Cell. *ACS Applied Materials & Interfaces* **2015**, *7* (4), 2286-2293.
- Kolomeisky, A. B.; Feng, X.; Krylov, A. I., A simple kinetic model for singlet fission: A role of electronic and entropic contributions to macroscopic rates. *The Journal of Physical Chemistry C* **2014**, *118* (10), S188-S195.
- Feng, X.; Kolomeisky, A. B.; Krylov, A. I., Dissecting the effect of morphology on the rates of singlet fission: Insights from theory. *The Journal of Physical Chemistry C* **2014**, *118* (34), 19608-19617.
- Matsika, S.; Feng, X.; Luzanov, A. V.; Krylov, A. I., What We Can Learn from the Norms of One-Particle Density Matrices, and What We Can't: Some Results for Interstate Properties in Model Singlet Fission Systems. *The Journal of Physical Chemistry A* **2014**, *118* (51), 11943-11955.
- Margulies, E. A.; Miller, C. E.; Wu, Y.; Ma, L.; Schatz, G. C.; Young, R. M.; Wasielewski, M. R., Enabling singlet fission by controlling intramolecular charge transfer in π -stacked covalent terylene-diimide dimers. *Nature Chemistry* **2016**, *8*, 1120.
- Sung, J.; Nowak-Król, A.; Schlosser, F.; Fimmel, B.; Kim, W.; Kim, D.; Würthner, F., Direct Observation of Excimer-Mediated Intramolecular Electron Transfer in a Cofacially-Stacked Perylene Bisimide Pair. *Journal of the American Chemical Society* **2016**, *138* (29), 9029-9032.
- Schrauben, J. N.; Akdag, A.; Wen, J.; Havlas, Z.; Ryerson, J. L.; Smith, M. B.; Michl, J.; Johnson, J. C., Excitation Localization/Delocalization Isomerism in a Strongly Coupled Covalent Dimer of 1,3-Diphenylisobenzofuran. *The Journal of Physical Chemistry A* **2016**, *120* (20), 3473-3483.
- Freeman, D. M. E.; Musser, A. J.; Frost, J. M.; Stern, H. L.; Forster, A. K.; Fallon, K. J.; Rapidis, A. G.; Cacialli, F.; McCulloch, I.; Clarke, T. M.; Friend, R. H.; Bronstein, H., Synthesis and Exciton Dynamics of Donor-Orthogonal Acceptor Conjugated Polymers: Reducing the Singlet-Triplet Energy Gap. *Journal of the American Chemical Society* **2017**, *139* (32), 11073-11080.
- Wu, Y.; Wang, Y.; Chen, J.; Zhang, G.; Yao, J.; Zhang, D.; Fu, H., Intramolecular Singlet Fission in an Antiaromatic Polycyclic Hydrocarbon. *Angewandte Chemie International Edition* **2017**, *56* (32), 9400-9404.
- Mauck Catherine, M.; Bae Youn, J.; Chen, M.; Powers - Riggs, N.; Wu, Y. L.; Wasielewski Michael, R., Charge - Transfer Character in a Covalent Diketopyrrolopyrrole Dimer: Implications for Singlet Fission. *ChemPhotoChem* **2017**, *2* (3), 223-233.
- Pace, N. A.; Zhang, W.; Arias, D. H.; McCulloch, I.; Rumbles, G.; Johnson, J. C., Controlling Long-Lived Triplet Generation from Intramolecular Singlet Fission in the Solid State. *The Journal of Physical Chemistry Letters* **2017**, *8* (24), 6086-6091.
- Sakuma, T.; Sakai, H.; Araki, Y.; Mori, T.; Wada, T.; Tkachenko, N. V.; Hasobe, T., Long-Lived Triplet Excited States of Bent-Shaped Pentacene Dimers by Intramolecular Singlet Fission. *The Journal of Physical Chemistry A* **2016**, *120* (11), 1867-1875.
- Zirzmeier, J.; Casillas, R.; Reddy, S. R.; Coto, P. B.; Lehnher, D.; Chernick, E. T.; Papadopoulos, I.; Thoss, M.; Tykewski, R. R.; Guldi, D. M., Solution-based intramolecular singlet fission in cross-conjugated pentacene dimers. *Nanoscale* **2016**, *8* (19), 10113-10123.
- Sanders, Samuel N.; Kumarasamy, E.; Pun, Andrew B.; Steigerwald, Michael L.; Sfeir, Matthew Y.; Campos, Luis M., Singlet Fission in Polypentacene. *Chem* **2016**, *1* (3), S05-S11.
- Cook, J. D.; Carey, T. J.; Damrauer, N. H., Solution-Phase Singlet Fission in a Structurally Well-Defined Norbornyl-Bridged Tetracene Dimer. *The Journal of Physical Chemistry A* **2016**, *120* (26), 4473-4481.
- Carey, T. J.; Snyder, J. L.; Miller, E. G.; Sammakia, T.; Damrauer, N. H., Synthesis of Geometrically Well-Defined Covalent Acene Dimers for Mechanistic Exploration of Singlet Fission. *The Journal of Organic Chemistry* **2017**, *82* (9), 4866-4874.
- Trinh, M. T.; Pinkard, A.; Pun, A. B.; Sanders, S. N.; Kumarasamy, E.; Sfeir, M. Y.; Campos, L. M.; Roy, X.; Zhu, X. Y., Distinct properties of the triplet pair state from singlet fission. *Science Advances* **2017**, *3* (7).
- Lehnher, D.; Alzola, J. M.; Mulzer, C. R.; Hein, S. J.; Dichtel, W. R., Diazatetracenes Derived from the Benzannulation of Acetylenes: Electronic Tuning via Substituent Effects and External Stimuli. *The Journal of Organic Chemistry* **2017**, *82* (4), 2004-2010.
- Liu, H.; Wang, R.; Shen, L.; Xu, Y.; Xiao, M.; Zhang, C.; Li, X., A Covalently Linked Tetracene Trimer: Synthesis and Singlet Exciton Fission Property. *Organic Letters* **2017**, *19* (3), 580-583.
- Kumarasamy, E.; Sanders, S. N.; Tayebjee, M. J. Y.; Asadpoordarwish, A.; Hele, T. J. H.; Fuemmeler, E. G.; Pun, A. B.; Yablou, L. M.; Low, J. Z.; Paley, D. W.; Dean, J. C.; Choi, B.; Scholes, G. D.; Steigerwald, M. L.; Ananth, N.; McCamey, D. R.; Sfeir, M. Y.; Campos, L. M., Tuning Singlet Fission in π -Bridge- π Chromophores. *Journal of the American Chemical Society* **2017**, *139* (36), 12488-12494.
- Pun Andrew, B.; Sanders Samuel, N.; Kumarasamy, E.; Sfeir Matthew, Y.; Congreve Daniel, N.; Campos Luis, M., Triplet Harvesting from Intramolecular Singlet Fission in Polytetracene. *Advanced Materials* **2017**, *29* (41), 1701416.
- Dean, J. C.; Zhang, R.; Hallani, R. K.; Pensack, R. D.; Sanders, S. N.; Oblinsky, D. G.; Parkin, S. R.; Campos, L. M.; Anthony, J. E.; Scholes, G. D., Photophysical characterization and time-resolved spectroscopy of an anthradithiophene dimer: exploring the role of conformation in singlet fission. *Physical Chemistry Chemical Physics* **2017**, *19* (34), 23162-23175.
- Cook, J. D.; Carey, T. J.; Arias, D. H.; Johnson, J. C.; Damrauer, N. H., Solvent-Controlled Branching of Localized versus Delocalized Singlet Exciton States and Equilibration with Charge Transfer in a Structurally Well-Defined Tetracene Dimer. *The Journal of Physical Chemistry A* **2017**, *121* (48), 9229-9242.
- Bettinger, H. F.; Einholz, R.; Gottler, A.; Junge, M.; Sattler, M.-S.; Schnepf, A.; Schrenk, C.; Schundelmeier, S.; Speiser, B., 6,6[prime or minute],11,11[prime or minute]-Tetra((triisopropylsilyl)ethynyl)-anti-[2.2](1,4)tetracenophane: a covalently coupled tetracene dimer and its structural, electrochemical, and photophysical characterization. *Organic Chemistry Frontiers* **2017**, *4* (5), 853-860.
- Wang, X.; Wang, R.; Shen, L.; Tang, Z.; Wen, C.; Dong, B.; Liu, H.; Zhang, C.; Li, X., Intramolecular singlet fission in a face-to-face stacked tetracene trimer. *Physical Chemistry Chemical Physics* **2018**, *20* (9), 6330-6336.
- Hetzer, C.; Guldi Dirk, M.; Tykewski Rik, R., Pentacene Dimers as a Critical Tool for the Investigation of Intramolecular Singlet Fission. *Chemistry - A European Journal* **2018**, *24*, 1-14.
- Carey, T. J.; Miller, E. G.; Gilligan, A. T.; Sammakia, T.; Damrauer, N. H., Modular Synthesis of Rigid Polyacene Dimers for Singlet Fission. *Organic Letters* **2018**, *20* (2), 457-460.
- Wang, L.; Wu, Y.; Chen, J.; Wang, L.; Liu, Y.; Yu, Z.; Yao, J.; Fu, H., Absence of Intramolecular Singlet Fission in Pentacene-Perylene-diimide Heterodimers:

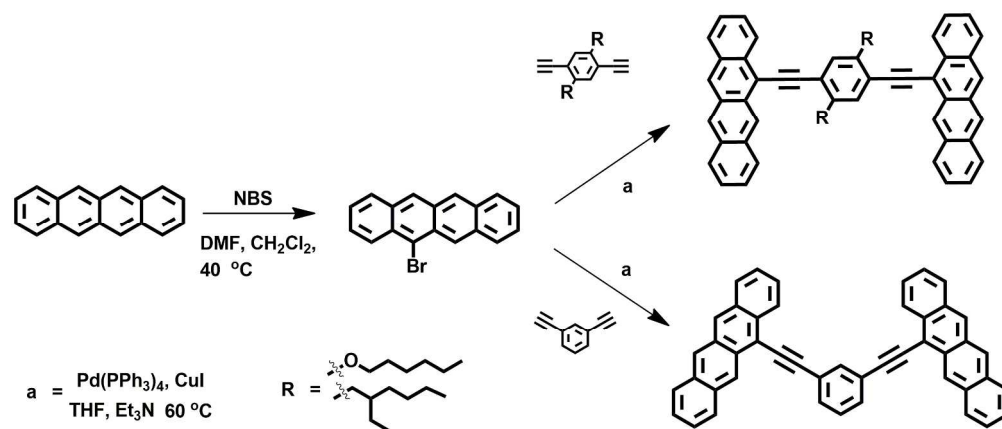
- The Role of Charge Transfer State. *The Journal of Physical Chemistry Letters* **2017**, *8*(22), 5609-5615.
35. Liu, H.; Wang, X.; Pan, L.; Shen, L.; Wang, X.; Chen, Q.; Li, X., Synthesis and photophysical properties of a bistetracene compound with slipped stacked structure. *Journal of Photochemistry and Photobiology A: Chemistry* **2017**, *340*, 21-28.
36. Yamakado, T.; Takahashi, S.; Watanabe, K.; Matsumoto, Y.; Osuka, A.; Saito, S., Conformational Planarization vs Singlet Fission: Distinct Excited - State Dynamics of Cyclooctatetraene - Fused Acene Dimers. *Angew. Chem. Int. Ed.* **2018**, *57*, 5438-5448.
37. Zirzmeier, J.; Lehnher, D.; Coto, P. B.; Chernick, E. T.; Casillas, R.; Basel, B. S.; Thoss, M.; Tykewski, R. R.; Guldi, D. M., Singlet fission in pentacene dimers. *Proceedings of the National Academy of Sciences* **2015**, *112*(17), 5325-5330.
38. Müller, A. M.; Avlasevich, Y. S.; Müllen, K.; Bardeen, C. J., Evidence for exciton fission and fusion in a covalently linked tetracene dimer. *Chem. Phys. Lett.* **2006**, *421*(4), 518-522.
39. Johnson, J. C.; Akdag, A.; Zamadar, M.; Chen, X.; Schwerin, A. F.; Paci, I.; Smith, M. B.; Havlas, Z.; Miller, J. R.; Ratner, M. A.; Nozik, A. J.; Michl, J., Toward Designed Singlet Fission: Solution Photophysics of Two Indirectly Coupled Covalent Dimers of 1,3-Diphenylisobenzofuran. *The Journal of Physical Chemistry B* **2013**, *117*(16), 4680-4695.
40. Müller, A. M.; Avlasevich, Y. S.; Schoeller, W. W.; Müllen, K.; Bardeen, C. J., Exciton fission and fusion in bis (tetracene) molecules with different covalent linker structures. *J. Am. Chem. Soc.* **2007**, *129*(46), 14240-14250.
41. Yamakado, T.; Takahashi, S.; Watanabe, K.; Matsumoto, Y.; Osuka, A.; Saito, S., Conformational Planarization versus Singlet Fission: Distinct Excited - State Dynamics of Cyclooctatetraene - Fused Acene Dimers. *Angewandte Chemie International Edition* **2018**, *57*(19), 5438-5443.
42. Grieco, C.; Kennehan, E. R.; Kim, H.; Pensack, R. D.; Brigeman, A. N.; Rimshaw, A.; Payne, M. M.; Anthony, J. E.; Giebink, N. C.; Scholes, G. D.; Asbury, J. B., Direct Observation of Correlated Triplet Pair Dynamics during Singlet Fission Using Ultrafast Mid-IR Spectroscopy. *The Journal of Physical Chemistry C* **2018**, *122*(4), 2012-2022.
43. Folie, B. D.; Haber, J. B.; Refaely-Abramson, S.; Neaton, J. B.; Ginsberg, N. S., Long-Lived Correlated Triplet Pairs in a π -Stacked Crystalline Pentacene Derivative. *Journal of the American Chemical Society* **2018**, *140*(6), 2326-2335.
44. Basel, B. S.; Zirzmeier, J.; Hetzer, C.; Reddy, S. R.; Phelan, B. T.; Krzyaniak, M. D.; Volland, M. K.; Coto, P. B.; Young, R. M.; Clark, T.; Thoss, M.; Tykewski, R. R.; Wasielewski, M. R.; Guldi, D. M., Evidence for Charge-Transfer Mediation in the Primary Events of Singlet Fission in a Weakly Coupled Pentacene Dimer. *Chem* **2018**, *4*(5), 1092-1111.
45. Hart, S.; Silva, W. R.; Frontiera, R. R., Femtosecond stimulated Raman evidence for charge-transfer character in pentacene singlet fission. *Chemical Science* **2018**, *9*(5), 1242-1250.
46. Ito, S.; Nagami, T.; Nakano, M., Design Principles of Electronic Couplings for Intramolecular Singlet Fission in Covalently-Linked Systems. *The Journal of Physical Chemistry A* **2016**, *120*(31), 6236-6241.
47. Zeng, T., Through-Linker Intramolecular Singlet Fission: General Mechanism and Designing Small Chromophores. *The Journal of Physical Chemistry Letters* **2016**, *7*(21), 4405-4412.
48. Feng, X.; Luzanov, A. V.; Krylov, A. I., Fission of entangled spins: An electronic structure perspective. *The Journal of Physical Chemistry Letters* **2013**, *4*(22), 3845-3852.
49. Korovina, N. V.; Das, S.; Nett, Z.; Feng, X.; Joy, J.; Haiges, R.; Krylov, A. I.; Bradforth, S. E.; Thompson, M. E., Singlet Fission in a Covalently Linked Cofacial Alkynyltetracene Dimer. *J. Am. Chem. Soc.* **2016**, *138*(2), 617-627.
50. Perkampus, H.; Sandeman, I.; Timmons, C., DMS UV Atlas of Organic Compounds, Verlag Chemie, Weinheim, Butterworths, London, England: 1966.
51. Pensack, R. D.; Tilley, A. J.; Parkin, S. R.; Lee, T. S.; Payne, M. M.; Gao, D.; Jahnke, A. A.; Oblinsky, D.; Li, P.-F.; Anthony, J. E., Exciton Delocalization Drives Rapid Singlet Fission in Nanoparticles of Acene Derivatives. *Journal of the American Chemical Society* **2015**, *137*, 6790-6803.
52. Murov, S. L.; Carmichael, I.; Hug, G. L., *Handbook of photochemistry*. CRC Press: 1993.
53. Sanders, S. N.; Kumarasamy, E.; Pun, A. B.; Trinh, M. T.; Choi, B.; Xia, J.; Taffet, E. J.; Low, J. Z.; Miller, J. R.; Roy, X.; Zhu, X. Y.; Steigerwald, M. L.; Sfeir, M. Y.; Campos, L. M., Quantitative Intramolecular Singlet Fission in Bipentacenes. *J. Am. Chem. Soc.* **2015**, *137*(28), 8965-8972.
54. Roberts, S. T.; McAnally, R. E.; Mastron, J. N.; Webber, D. H.; Whited, M. T.; Brutchey, R. L.; Thompson, M. E.; Bradforth, S. E., Efficient singlet fission discovered in a disordered acene film. *Journal of the American Chemical Society* **2012**, *134*(14), 6388-6400.
55. Reusswig, P. D.; Congreve, D. N.; Thompson, N. J.; Baldo, M. A., Enhanced external quantum efficiency in an organic photovoltaic cell via singlet fission exciton sensitizer. *Appl. Phys. Lett.* **2012**, *101*(11), 113304.
56. Rolczynski, B. S.; Szarko, J. M.; Son, H. J.; Liang, Y.; Yu, L.; Chen, L. X., Ultrafast intramolecular exciton splitting dynamics in isolated low-band-gap polymers and their implications in photovoltaic materials design. *Journal of the American Chemical Society* **2012**, *134*(9), 4142-4152.
57. Roberts, S. T.; Schlenker, C. W.; Barlier, V.; McAnally, R. E.; Zhang, Y.; Mastron, J. N.; Thompson, M. E.; Bradforth, S. E., Observation of triplet exciton formation in a platinum-sensitized organic photovoltaic device. *The Journal of Physical Chemistry Letters* **2010**, *2*(2), 48-54.
58. Ryerson, J. L.; Schrauben, J. N.; Ferguson, A. J.; Sahoo, S. C.; Naumov, P.; Havlas, Z.; Michl, J.; Nozik, A. J.; Johnson, J. C., Two Thin Film Polymorphs of the Singlet Fission Compound 1,3-Diphenylisobenzofuran. *The Journal of Physical Chemistry C* **2014**, *118*(23), 12121-12132.
59. Ryerson, J. L.; Schrauben, J. N.; Ferguson, A. J.; Sahoo, S. C.; Naumov, P. e.; Havlas, Z. k.; Michl, J.; Nozik, A. J.; Johnson, J. C., Two Thin Film Polymorphs of the Singlet Fission Compound 1, 3-Diphenylisobenzofuran. *The Journal of Physical Chemistry C* **2014**, *118*(23), 12121-12132.
60. Thompson, N. J.; Wilson, M. W.; Congreve, D. N.; Brown, P. R.; Scherer, J. M.; Bischof, T. S.; Wu, M.; Geva, N.; Welborn, M.; Van Voorhis, T., Energy harvesting of non-emissive triplet excitons in tetracene by emissive PbS nanocrystals. *Nature materials* **2014**, *13*, 1039-1043.
61. Thorsmølle, V. K.; Averitt, R. D.; Damsar, J.; Smith, D.; Tretiak, S.; Martin, R.; Chi, X.; Crone, B.; Ramirez, A.; Taylor, A., Morphology effectively controls singlet-triplet exciton relaxation and charge transport in organic semiconductors. *Phys. Rev. Lett.* **2009**, *102*(1), 017401.
62. Müller, A. M.; Avlasevich, Y. S.; Schoeller, W. W.; Müllen, K.; Bardeen, C. J., Exciton Fission and Fusion in Bis(tetracene) Molecules with Different Covalent Linker Structures. *Journal of the American Chemical Society* **2007**, *129*(46), 14240-14250.
63. Feng, X.; Krylov, A. I., On couplings and excimers: lessons from studies of singlet fission in covalently linked tetracene dimers. *Physical Chemistry Chemical Physics* **2016**, *18*(11), 7751-7761.
64. Feng, X.; Casanova, D.; Krylov, A. I., Intra- and Intermolecular Singlet Fission in Covalently Linked Dimers. *The Journal of Physical Chemistry C* **2016**, *120*(34), 19070-19077.
65. Abraham, V.; Mayhall, N. J., Simple Rule To Predict Boundedness of Multiexciton States in Covalently Linked Singlet-Fission Dimers. *The Journal of Physical Chemistry Letters* **2017**, *8*(22), 5472-5478.
66. Sonogashira, K., Development of Pd-Cu catalyzed cross-coupling of terminal acetylenes with sp²-carbon halides. *Journal of Organometallic Chemistry* **2002**, *653*(1), 46-49.
67. Yost, S. R.; Lee, J.; Wilson, M. W. B.; Wu, T.; McMahan, D. P.; Parkhurst, R. R.; Thompson, N. J.; Congreve, D. N.; Rao, A.; Johnson, K.; Sfeir, M. Y.; Bawendi, M.; Swager, T. M.; Friend, R. H.; A, M.; van Voorhis, T., *Nat. Chem.* **2014**, *6*, 492.
68. Grabowski, Z. R.; Rotkiewicz, K.; Rettig, W., Structural Changes Accompanying Intramolecular Electron Transfer: Focus on Twisted Intramolecular Charge-Transfer States and Structures. *Chemical Reviews* **2003**, *103*(10), 3899-4032.
69. Berkelbach, T. C.; Hybertsen, M. S.; Reichman, D. R., Microscopic theory of singlet exciton fission. II. Application to pentacene dimers and the role of superexchange. *The Journal of Chemical Physics* **2013**, *138*(11), 114103.
70. Lukman, S.; Musser, A. J.; Chen, K.; Athanasopoulos, S.; Yong, C. K.; Zeng, Z.; Ye, Q.; Chi, C.; Hodgkiss, J. M.; Wu, J.; Friend, R. H.; Greenham, N. C., Tuneable Singlet Exciton Fission and Triplet-Triplet Annihilation in an Orthogonal Pentacene Dimer. *Adv. Funct. Mater.* **2015**, *25*(34), 5452-5461.
71. Lippitz, M.; Hübner, C. G.; Christ, T.; Eichner, H.; Bordat, P.; Herrmann, A.; Müllen, K.; Basché, T., Coherent Electronic Coupling versus Localization in Individual Molecular Dimers. *Phys. Rev. Lett.* **2004**, *92*(10), 103001.
72. Nguyen, M.-H.; Nguyen, V. H.; Yip, J. H., Sequence-Specific Synthesis of Platinum-Conjugated Trichromophoric Energy Cascades of Anthracene, Tetracene, and Pentacene and Fluorescent "Black Chromophores". *Organometallics* **2013**, *32*(24), 7283-7291.

73. Burdett, J. J.; Bardeen, C. J., The dynamics of singlet fission in crystalline tetracene and covalent analogs. *Accounts of chemical research* **2013**, *46* (6), 1312-1320.
74. Arias, D. H.; Ryerson, J. L.; Cook, J. D.; Damrauer, N. H.; Johnson, J. C., Polymorphism influences singlet fission rates in tetracene thin films. *Chemical Science* **2016**, *7*(2), 1185-1191.
75. Marciniak, H.; Pugliesi, I.; Nickel, B.; Lochbrunner, S., Ultrafast singlet and triplet dynamics in microcrystalline pentacene films. *Physical Review B* **2009**, *79* (23), 235318.
76. Montalti, M.; Credi, A.; Prodi, L.; Gandolfi, M. T., *Handbook of Photochemistry*. 3 ed.; Boca Raton, Florida, 2006.
77. McQuade, D. T.; Pullen, A. E.; Swager, T. M., *Chem. Rev.* **2000**, *100*, 2537.
78. van Stokkum, I. H. M.; Larsen, D. S.; van Grondelle, R., Global and target analysis of time-resolved spectra. *Biochimica et Biophysica Acta (BBA) - Bioenergetics* **2004**, *1657*(2), 82-104.
79. McQuade, D. T.; Kim, J.; Swager, T. M., *J. Am. Chem. Soc.* **2000**, *122*, 5885.
80. Van Dyke, D. A.; Pryor, B. A.; Smith, P. G.; Topp, M. R., Nanosecond Time-Resolved Fluorescence Spectroscopy in the Physical Chemistry Laboratory: Formation of the Pyrene Excimer in Solution. *Journal of Chemical Education* **1998**, *75* (5), 615.
81. Giaimo, J. M.; Lockard, J. V.; Sinks, L. E.; Scott, A. M.; Wilson, T. M.; Wasielewski, M. R., Excited singlet states of covalently bound, cofacial dimers and trimers of perylene-3, 4: 9, 10-bis (dicarboximide) s. *The Journal of Physical Chemistry A* **2008**, *112* (11), 2322-2330.
82. Miller, C. E.; Wasielewski, M. R.; Schatz, G. C., Modeling Singlet Fission in Rylene and Diketopyrrolopyrrole Derivatives: The Role of the Charge Transfer State in Superexchange and Excimer Formation. *The Journal of Physical Chemistry C* **2017**, *121* (19), 10345-10350.
83. Breen, I.; Tempelaar, R.; Bizimana, L. A.; Kloss, B.; Reichman, D. R.; Turner, D. B., Triplet Separation Drives Singlet Fission after Femtosecond Correlated Triplet Pair Production in Rubrene. *Journal of the American Chemical Society* **2017**, *139* (34), 11745-11751.
84. Hetzer, C.; Guldi Dirk, M.; Tykwinski Rik, R., Pentacene Dimers as a Critical Tool for the Investigation of Intramolecular Singlet Fission. *Chemistry & A European Journal* **2018**, *0*(0).
85. Monahan, N.; Zhu, X. Y., Charge Transfer-Mediated Singlet Fission. *Annual Review of Physical Chemistry* **2015**, *66* (1), 601-618.
86. Zimmerman, P. M.; Bell, F.; Casanova, D.; Head-Gordon, M., Mechanism for singlet fission in pentacene and tetracene: From single exciton to two triplets. *Journal of the American Chemical Society* **2011**, *133* (49), 19944-19952.
87. Aryanpour, K.; Shukla, A.; Mazumdar, S., Theory of Singlet Fission in Polyenes, Acene Crystals, and Covalently Linked Acene Dimers. *The Journal of Physical Chemistry C* **2015**, *119* (13), 6966-6979.
88. Beljonne, D.; Yamagata, H.; Brédas, J. L.; Spano, F. C.; Olivier, Y., Charge-Transfer Excitations Steer the Davydov Splitting and Mediate Singlet Exciton Fission in Pentacene. *Physical Review Letters* **2013**, *110* (22), 226402.
89. Liu, H.; Wang, Z.; Wang, X.; Shen, L.; Zhang, C.; Xiao, M.; Li, X., Singlet exciton fission in a linear tetracene tetramer. *Journal of Materials Chemistry C* **2018**, *6* (13), 3245-3253.
90. Tayebjee, M. J. Y.; Sanders, S. N.; Kumarasamy, E.; Campos, L. M.; Sfeir, M. Y.; McCamey, D. R., Quintet multiexciton dynamics in singlet fission. *Nature Physics* **2016**, *13*, 182.
91. Joy, J.; Korovina, N. V.; Thompson, M. E.; Bradforth, S. E., Decoupling Inter- and Intra- dimer singlet fission. *Proc. SPIE 10348, Physical Chemistry of Semiconductor Materials and Interfaces XVI* **2017**.

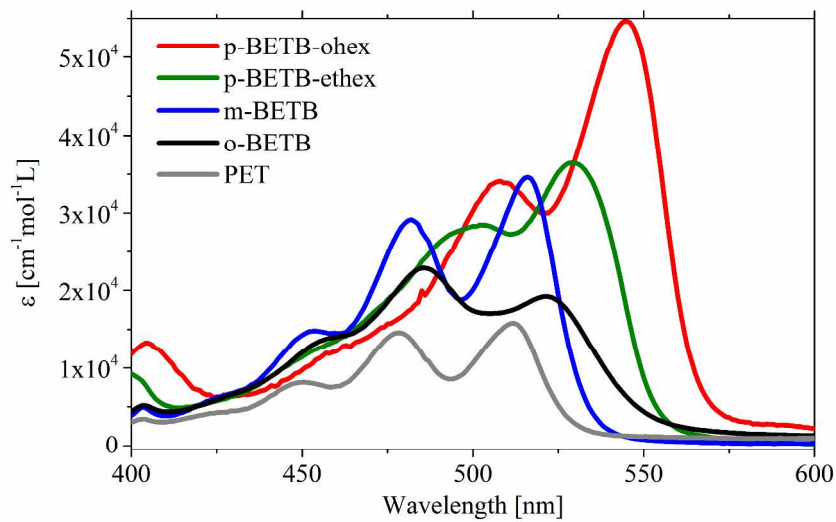




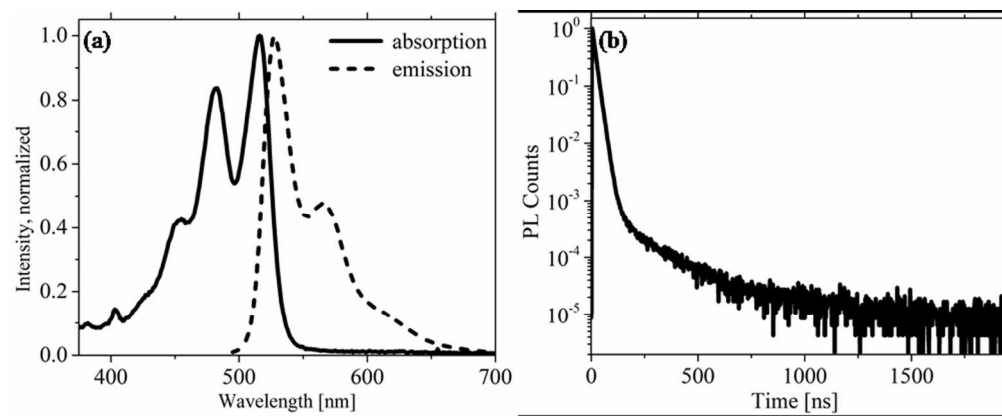
434x209mm (96 x 96 DPI)



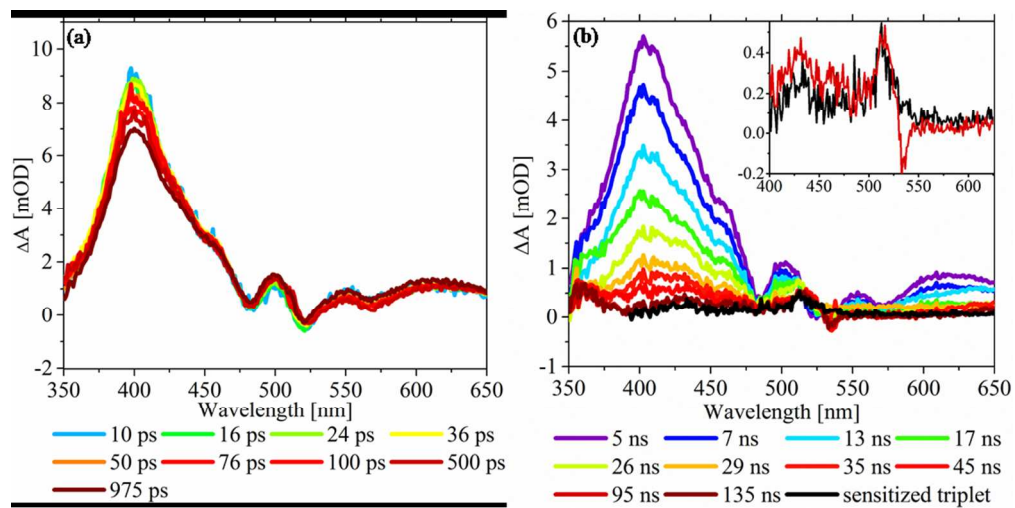
227x96mm (300 x 300 DPI)



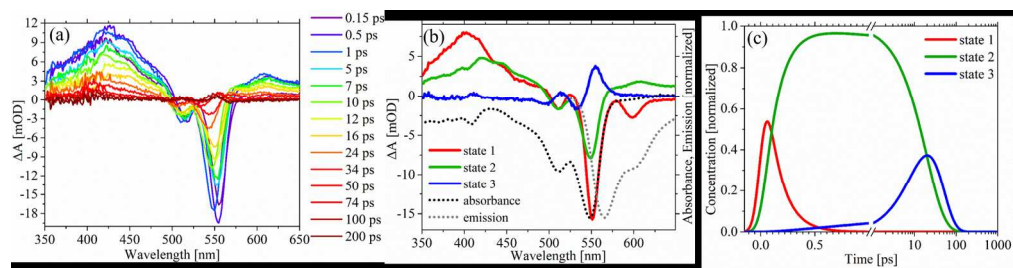
381x228mm (300 x 300 DPI)



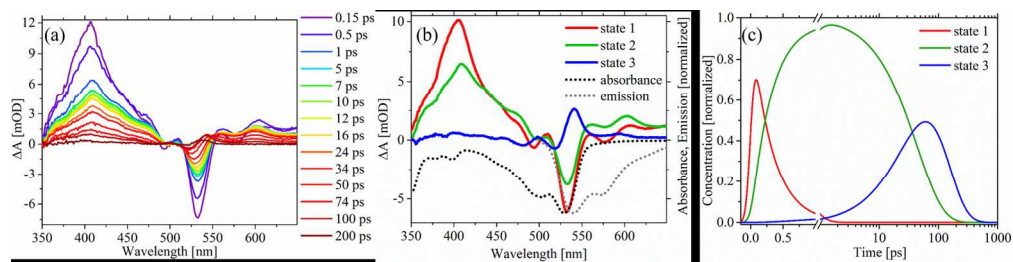
264x107mm (96 x 96 DPI)



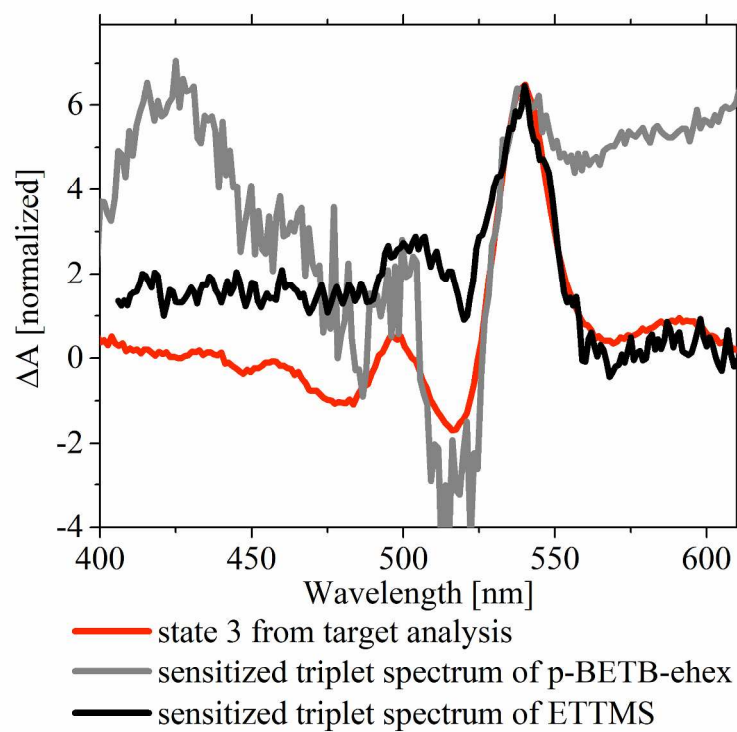
301x149mm (96 x 96 DPI)



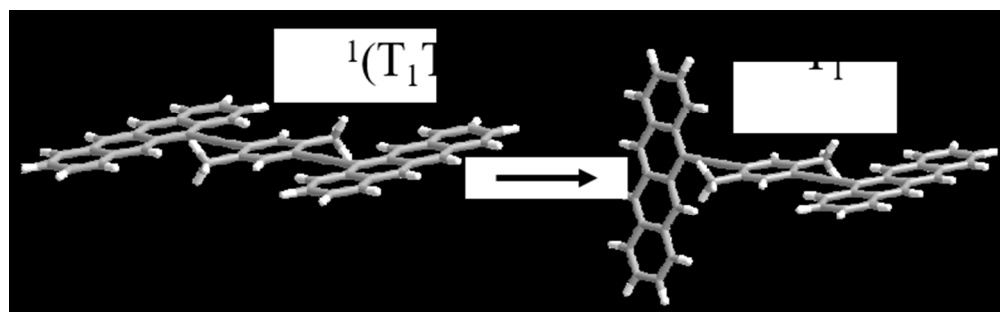
529x136mm (96 x 96 DPI)



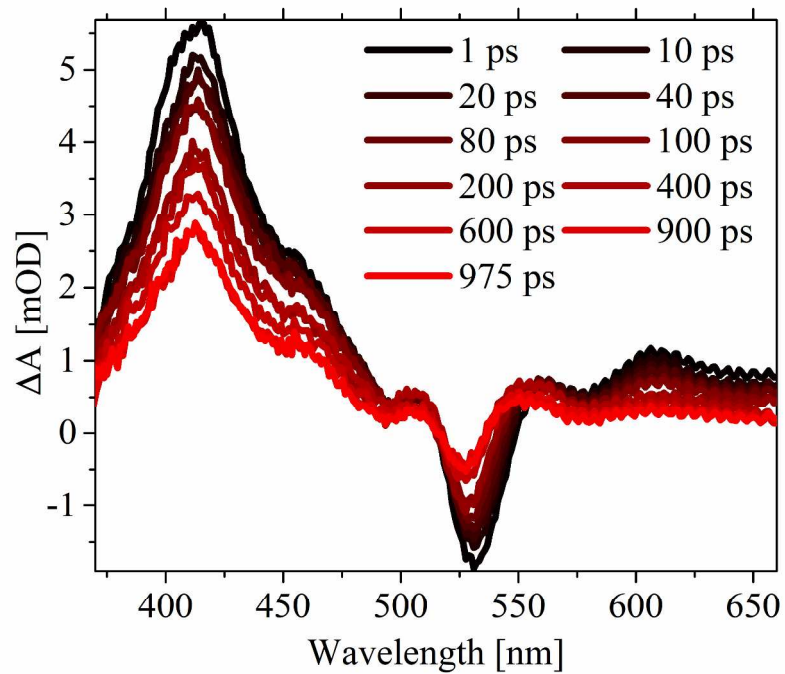
522x130mm (96 x 96 DPI)



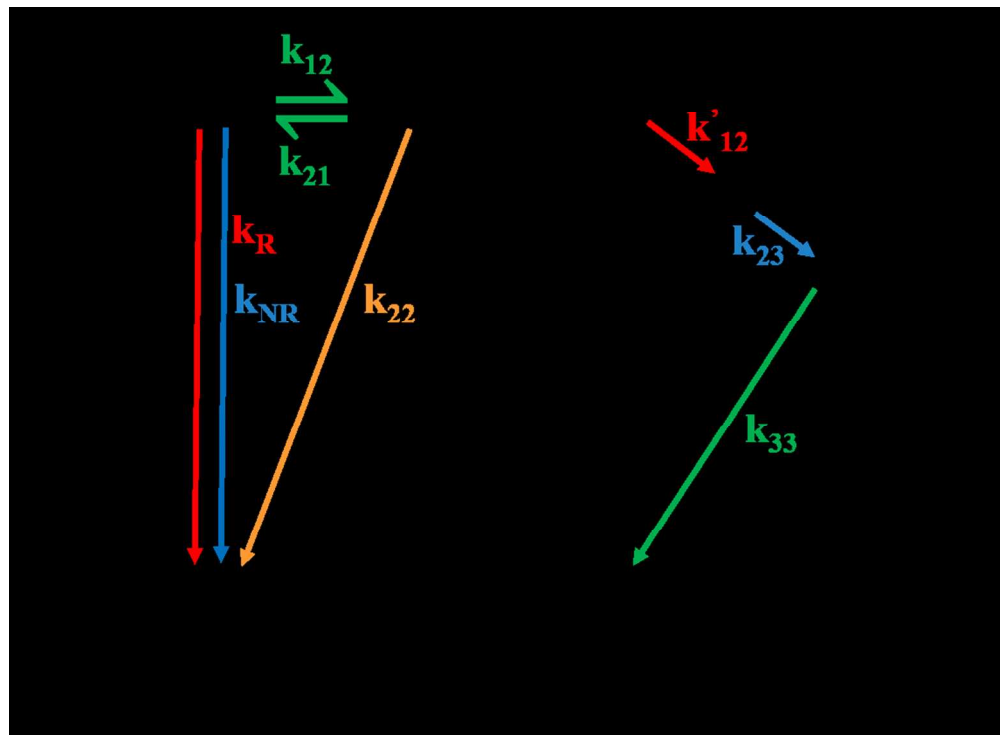
269x207mm (300 x 300 DPI)



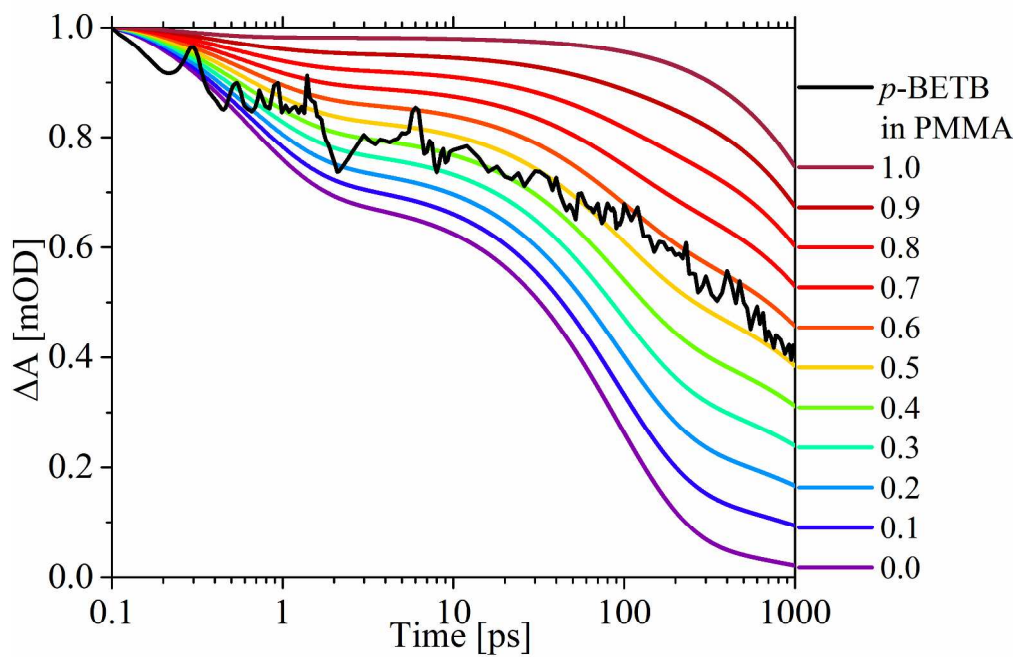
210x64mm (96 x 96 DPI)



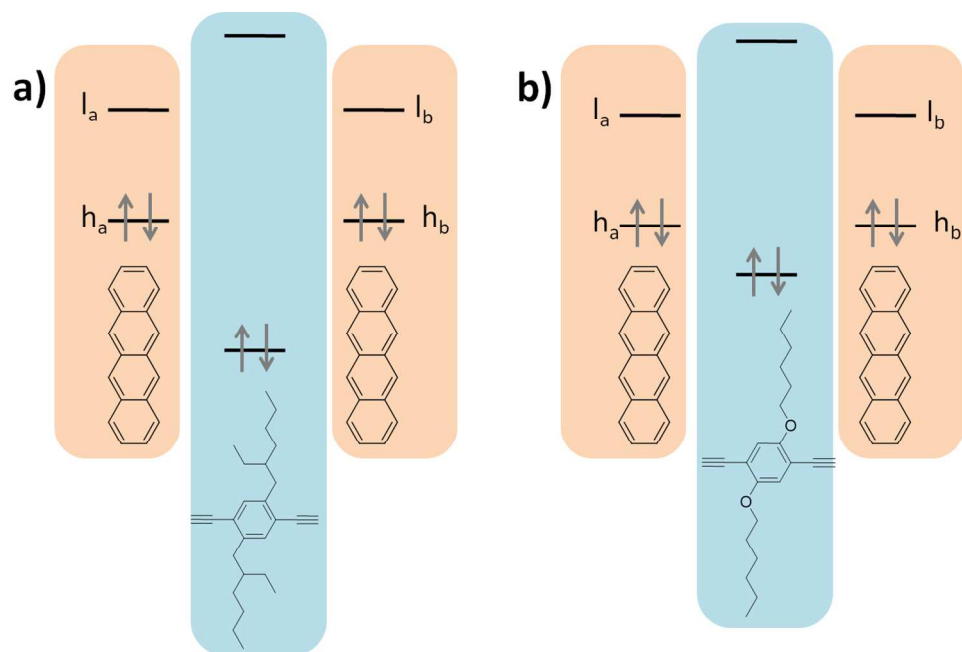
269x207mm (300 x 300 DPI)



303x222mm (96 x 96 DPI)



271x207mm (300 x 300 DPI)



388x249mm (96 x 96 DPI)